REACTION OF ZINC PROTEOME WITH BIOLOGICALLY IMPORTANT METAL BINDING LIGANDS

by

Kaniz Fatema

A Thesis Submitted in

Partial Fulfillment of the

Requirements for the Degree of

Master of Science

in Chemistry

at

The University of Wisconsin-Milwaukee

December 2015

ABSTRACT

REACTION OF ZINC PROTEOME WITH BIOLOGICALLY IMPORTANT METAL BINDING LIGANDS

by

Kaniz Fatema

The University of Wisconsin-Milwaukee, 2015
Under the Supervision of Distinguished Professor David H. Petering, Ph.D.

Abstract

Fluorescent sensors have been widely used as microscopic tools to image Zn^{2+} on a cellular level. Recently, it has been established that the sensors TSQ and Zinquin form adducts with Zn-proteins and image fractions of the Zn-proteome.[1] Since TSQ and Zinquin bind specifically to many Zn-proteins, it is hypothesized that other metal binding ligands, both synthetic and natural, may also bind to the Zn-proteome. Biologically active 1,10-phenanthroline (Phen) and related molecules were investigated for their ability to bind to Zn-proteome. Similarly, the cellular tripeptide, glutathione was investigated. It was observed that Phen and some other metal binding, bidentate ligands, were able to displace TSQ from the TSQ-Zn-proteome. Specifically when cellular Zn-proteome reacted with TSQ, adduct formation occurs, that was detected by fluorescence emission at 470 nm. Upon reaction of TSQ-Zn-proteome with 1,10-phenanthroline, glutathione, and some other related small molecules, a significant decrease in fluorescence was observed, indicating the displacement of TSQ by each competing ligand. Native SDS (NDS) PAGE electrophoresis of the product of the reaction of 1,10-Phenanthroline with TSQ-Zn-proteome further confirmed the displacement of TSQ from an array of Zn-proteins. This reaction was further characterized with the use of Zn-alcohol dehydrogenase as a model enzyme that reacts with TSQ and Phen. These studies reveal the Zn-proteome as widely available

for adduct formation at its zinc binding sites. The importance of such reactions is being investigated.

TABLE OF CONTENTS

LIST OF FIGURES

LIST OF ABBREVIATIONS

AAS	Flame Atomic Absorption Spectroscopy
AU	Arbitrary Units
ADH	Alcohol Dehydrogenase
BN-PAGE	Blue Native – Poly Acryl Amide Gel Electrophoresis
DPBS	Dulbecco's Poly Acryl Amide Gel Electrophoresis
FCS	Fetal Calf Serum
GSH	Glutathione
LMW	Low Molecular Weight
HMW	High Molecular Weight
MOPS	3-(*N*-morpholino)propanesulfonic acid
MTT	3(4,5-dimethyl-2-thiazoyl)-2,5-diphenyl-2*H*-tetrazolium bromide
NSDS-PAGE	Native Sodium Dodecyl Sulfate-Polyacrylamide Gel Electrophoresis
SDS	Sodium Dodecyl Sulfate
SOD	Superoxide Dismutase
TPEN	*N,N,N',N'*-Tetrakis(2-pyridylmethyl)ethylenediamine
ZQACID	(2-methyl-8-*p*-toluenesulfonamido-6-quinolyloxy)acetate
ZQEE	ethyl (2-methyl-8-*p*-toluenesulfonamido-6-quinolyloxy)acetate

Acknowledgements

Thank you very much to my parents for their support and love in my academic endeavors all the way until my graduation.

A sincere thanks to my advisor Dr. David H. Petering, for all his suggestions and advice during continuing this project and be patient to me with many ups and downs along the way through carrying out this research project. I am humbled for all his help.

I am thankful to Sue for all your help in the lab and I enjoyed working with all my colleagues Reza, Mohammad and Drew for training me and sharing me their ideas in many ways during the time of carrying out this research project to be successful.

Thank you,

Kaniz Fatema

1. Introduction

1.1. Zinc - its biological importance and regulation in the living organisms

Metal ions play pivotal roles in most biochemical processes.[2–8] In fact, many proteins bind to one or more metal ions to perform their functions. Such proteins are called metalloproteins.[2] The incorporation of the metal ions is very critical because either the metal ions play a role in the catalytic mechanism or because they determine or stabilize protein tertiary or quaternary structure.[2] The intracellular concentration of metals as well as their distribution among the various cell compartments and their incorporation into metalloproteins are tightly controlled.[9] The equilibria of the metal ions involved in the body and their proper control processes are necessary to maintain a healthy phenotype.

Zn^{2+} is one of the biologically essential metal ions that is a key element in all forms of life.[1,4,6–8,10,11] It is the second most abundant divalent transition metal ion in living organisms after iron. According to bioinformatics analysis, about 10% of the human genome has been proposed to encode Zn-binding proteins.[5,12] This translates into about 3000 Zn-binding proteins that populate in the mammalian proteome.[1,8,13–15] Zn^{2+} is involved in a wide range of protein function; it participates in more than 300 cellular processes such as DNA transcription, protein synthesis, neurotransmission, intracellular signaling, and antibiotic activities. [6,16]

There are two types of zinc binding sites in the intracellular environment, Zn^{2+} tightly bound to metalloproteins and also mobile forms of Zn^{2+}.[17]

Zinc is involved in the function of proteins, it participates in the control of cellular metabolism and signaling.[13] Roles of zinc ions in biological phosphorylation and in redox signaling are already well documented and are part of the spectrum of actions of zinc in cellular proliferation, differentiation, and cell death.[18] There are at least three areas that relate to the mobilization of zinc ions (i) exocytotic vesicles, (ii) intracellular organelles, and (iii) zinc/thiolate coordination environments of proteins by oxidation of the sulphur donor(s) of ligands.[13] Zinc is also used as a metal cofactor in proteins much more frequently than most vitamins. The control of a fluctuating pool of Zn^{2+} ions at remarkably low concentrations and with the participation of many proteins provide a new perspective on the molecular functions of zinc in biology in general and for the impact of zinc on human health in particular.[19]

The mobile forms of Zn^{2+} are thought to play vital roles in biosignaling. For example, due to the abundance of Zn^{2+} in the brain Zn^{2+} may serve as a neurotransmitter in the brain.[1] Disruption of transition metal homeostasis in human is involved with pathological conditions in brain, liver and kidney. Fe, Cu, and Zn dysregulation has been hypothesized to be associated with Alzheimer disease.[20,21,22] Zn deficiency and dyshomeostasis are associated with chronic diseases such as metabolic syndrome, diabetes and related complications, bone loss, growth retardation in young children, and neurological and behavioral problems.[22,18]

1.2. Protein Bound Zinc

When the entire human genome was scanned for zinc binding signatures among protein sequences, it was roughly suggested that about 3% of the genes encode zinc proteins.[8,11] But from other bioinformatics results, it has been rather strongly predicted that around 10% of

the human genome encodes zinc proteins.[11] This corresponds to about 2800 of human proteins that are potentially zinc-binding proteins *in vivo*.[2,8] The estimated number of zinc proteins in the human zinc proteome demonstrates that there is a widespread use of zinc in protein structure and function.[8] Among transition metals, Zn after iron is the most abundant transition metal in the human body and the most abundant metal in the brain.[23] The number of known zinc proteins include, 397 hydrolases, 302 ligases, 167 transferases, 43 oxidoreductase, 24 lysases, 957 transcription factors, 221 signaling proteins, 141 transport/storage proteins, 53 proteins with structural metal sites, 19 proteins in DNA repair, replication and translation, 427 zinc finger proteins, 456 proteins of unknown function (see Figure 1) .[8,11]

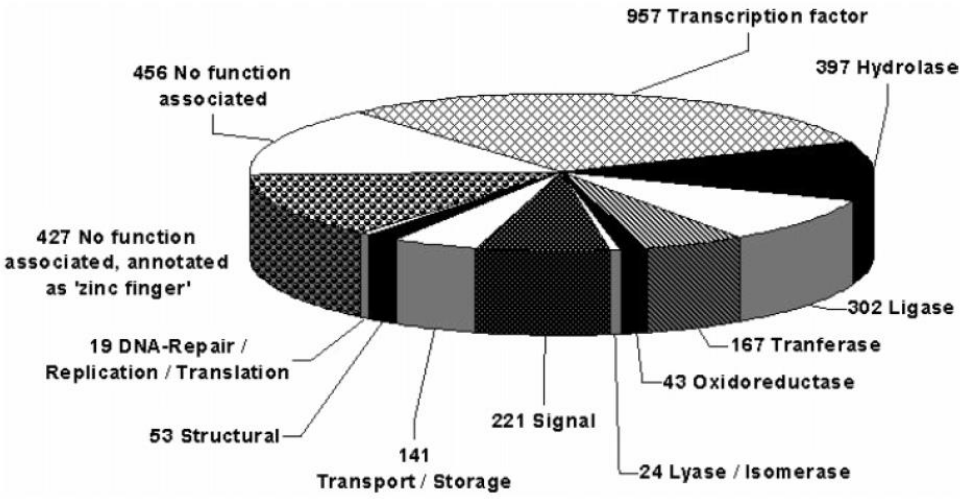

Figure 1.1: **Functional classification of all human zinc-proteins**. Most zinc fingers are included among transcription factors. 427 zinc fingers that are not annotated have been separately maintained.[11]

The eukaryotic Zn-proteome consists of two major groups of comparable sizes of zinc proteins: enzymes and transcription factors.[4] Available functional information suggests that the

large majority of human zinc-binding proteins are involved in the regulation of gene expression.[4,8,24] The most abundant class of zinc-binding proteins in human is that of zinc-fingers, with Cys_4 and Cys_2His_2 being the most common types of zinc coordination environment.[2]

Zinc binds as a cofactor to many proteins with a predominant preference of a tetrahedral coordination structure by four ligands. It most often bound by sulfur and nitrogen from cysteine and histidine, respectively, and to a lesser extent by oxygen from aspartate and glutamate.[1,8,11,24–27] Primarily Zn^{2+} ions are found in the form of mononuclear complexes and structures. In addition, zinc clusters are seen in enzymes such as metallothionein[28,26] In zinc enzymes the necessity for flexibility of the catalytic site toward its substrate leads to the more dynamic coordination of zinc by ligands from side chains of the protein. Examples are shown in Figure 1.2.

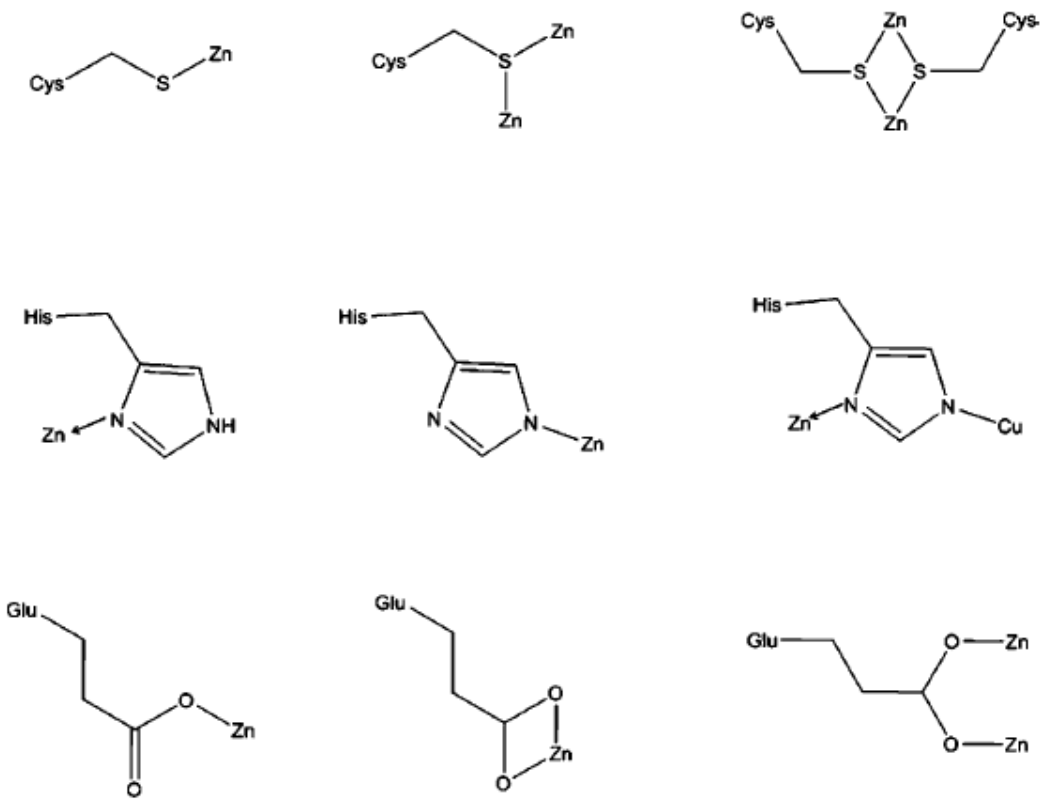

Figure 1.2: The interaction of zinc with ligands.

With few exceptions, zinc ligands in proteins are cysteine (Cys) (S-donor, histidine (His) (N-donor), or glutamate (Glu)/aspartate (Asp) (O-donor). For cysteine, there is a single mode of interaction. For histidine, binding occurs with either one of the two nitrogen atoms of the imidazole ring. For glutamate/aspartate, binding modes include one oxygen, which can be syn or anti (not shown), or both oxygen of the carboxylate. All three ligands can bridge one or several zinc ions. For cysteine, there are three bridges. An example of three bridges is the Zn_4S_{11} cluster of metallothionein. For histidine, the only bridges known are those between zinc and copper in superoxide dismutase (SOD1) and between zinc and zinc in the zinc transporter CzrB (*Thermus thermophiles*). Aspartate/glutamate can form a bridge with the two oxygens of the carboxylate,

for example in alkaline phosphatase and leucine aminopeptidase are referred to the motifs of zinc binding sites as "cocatalytic" or "coactive" .[11, 29]

NAD(P)-dependent oxidoreductases occur in virtually all organisms and catalyze the reversible oxidation of primary and secondary alcohols into aldehydes and ketones, respectively.[28] The first evidence of coordination dynamics in zinc enzymes stemmed from studies of zinc-dependent horse liver alcohol dehydrogenase (HL) ADH, a member of the family of medium-chain dehydrogenases/reductases.[30, 31] The ADHs in higher eukaryotes (plants and animals) are usually dimeric, whereas those in prokaryotes and lower eukaryotes (yeast) are tetrameric. In our study, we used a species of yeast alcohol dehydrogenase from *Saccharomyces cerevisiae.* The structure yeast ADH has been determined.[28] Each subunit of yeast ADH in the crystal contains a 'catalytic' zinc and a 'structural' zinc with no known functional role.[28] The protein ligands of the 'catalytic' zinc ion are two cysteines and one histidine. Additionally, four cysteines bind a second, structural zinc ion relatively far away from the active site. In ADH, coenzyme (NAD^+/NADH) binding induces conformational changes of the protein and alters the structure of the catalytic metal ion.[11]

1.3. Zn^{2+} trafficking

In order to understand the critical roles of Zn^{2+} in signaling, it is of utmost importance to know how metal ions become specifically distributed under steady-state conditions and temporally redistributed within the cell among the metal-binding structures during signaling processes. For these reasons the research area of Zn^{2+} trafficking has risen to the forefront of metallo-biochemistry over the past few decades.

In recognizing Zn^{2+} as a transient metabolite, it is implied that the concentration of reactive Zn^{2+} changes under different circumstances. This pool of Zn^{2+} might represent free Zn^{2+} or may stay bound to the proteome. In general, the metabolically active Zn^{2+} within the cells can be described as follows.

$$Zn^{2+} + L_1 \leftrightarrows Zn\text{-}L_1 \quad (1.1)$$

$$Zn\text{-}L_1 + L_2 \leftrightarrows Zn\text{-}L_2 + L_1 \ldots\ldots\ldots\ldots Zn\text{-}L_n + L_{n-1} \quad (1.2)$$

In general, the Zn^{2+} ions that participate in these cellular reactions are considered to be mobile; that is, they are able to move among ligands. Typically the status of mobile Zn^{2+} in the cellular environment can be termed as, “exchangeable”, “chelatable”, “labile”, or “free” Zn^{2+}.[32,1,33,34] Increased understanding of these reactions has been envisioned in many research studies through the application of many experimental tools which have been employed to monitor and assess the facets of the Zn^{2+} status of the cellular environment.

Studies of the transient Zn^{2+} is particularly difficult due to the filled d^{10} electronic structure. That makes Zn^{2+} invisible to visible electronic spectroscopy and paramagnetic methods. Therefore, the common methods to study iron and copper, for example, can not equally be employed to investigate Zn^{2+}. These limitations have led researchers to develop other tools to monitor cellular zinc distribution and function. The cell permeable fluorescent probes have been designed over the past two decades to study cellular zinc. The objectives are to be able to observe cellular Zn^{2+} trafficking, mobilization and signalling using such zinc reactive fluorophores.[33]

1.4. The zinc sensors

Fluorescent zinc sensors are compounds that undergo a change in fluorescence emission in the presence of Zn^{2+}. Fluorescence imaging has proven to be an attractive suitable technique for in vivo monitoring.[35] Some examples of zinc fluorophores are shown in Figure 1.3. These Zn^{2+} sensors have been the widely used tool to study Zn^{2+} in the cellular environment. It has been assumed that these sensors exhibit fluorescence changes when interacting with free Zn^{2+} within the cell.

$$Zn^{2+} + \text{sensor (S)} \leftrightarrows \text{Zn-sensor (Zn-S)} \quad (1.3)$$

Intracellular changes in the free Zn^{2+} may be evaluated by monitoring fluorescence changes after a given stimulus. The zinc sensors function properly only in the condition when the equilibrium constant (K) of the reaction would lie within the range of transient Zn^{2+} concentration and the concentration of Zn-S emits enough fluorescence to be observable. When a sensor binds Zn^{2+} poorly, the change in fluorescence is insufficient to detect the free Zn^{2+} concentration. Moreover, mobilized Zn^{2+} may bind to adventitous sites within the proteome and among small molecules.

$$Zn + L_{AS} \leftrightarrows Zn\text{-}L_{AS} \quad (1.4)$$

Depending on the equilibrium constants the sensor and these other molecules for Zn^{2+}, sensor will bind and detect Zn^{2+} in this pool.

$$\sum Zn\text{-}L + S \leftrightarrows Zn\text{-}S + \sum L \quad (1.5)$$

Moreover, when the sensor binds strongly to Zn^{2+} it may chelate zinc from its non-transient Zn-protein pool. Therefore, a more accurate representation of the chemistry involved in Zn-sensor investigation can be described as follows.

$$\sum \text{Zn-Protein} + \text{sensor} \leftrightarrows \text{Zn-sensor} + \sum \text{Protein} \quad (1.6)$$

The extent to which the sensor interacts with the non-transient Zn^{2+} pool is again associated with the thermodynamic and kinetic properties of the sensor and the Zn-proteins. These interactions must be minimal in order to draw any conclusion about the changes in the transient Zn^{2+}.

One of the most commonly used fluorophores and first to be commercially available is 6-methoxy-(8-p-toluenesulfonamido)quinoline or TSQ. It was first developed as a histochemical stain for Zn^{2+} in brain tissue.[36,37] TSQ is one of the specific fluorescent probes that gives fluorescence emission only with Zn^{2+}. This very selective character of sensing Zn^{2+} makes TSQ an excellent choice to use as a reporter for Zn^{2+} trafficking tool. TSQ binds with Zn^{2+} and makes a complex in a 2:1 stoichiometric ratio, resulting in the conversion of the non-fluorescent TSQ molecule into a strongly fluorescent Zn^{2+} complex.[1]

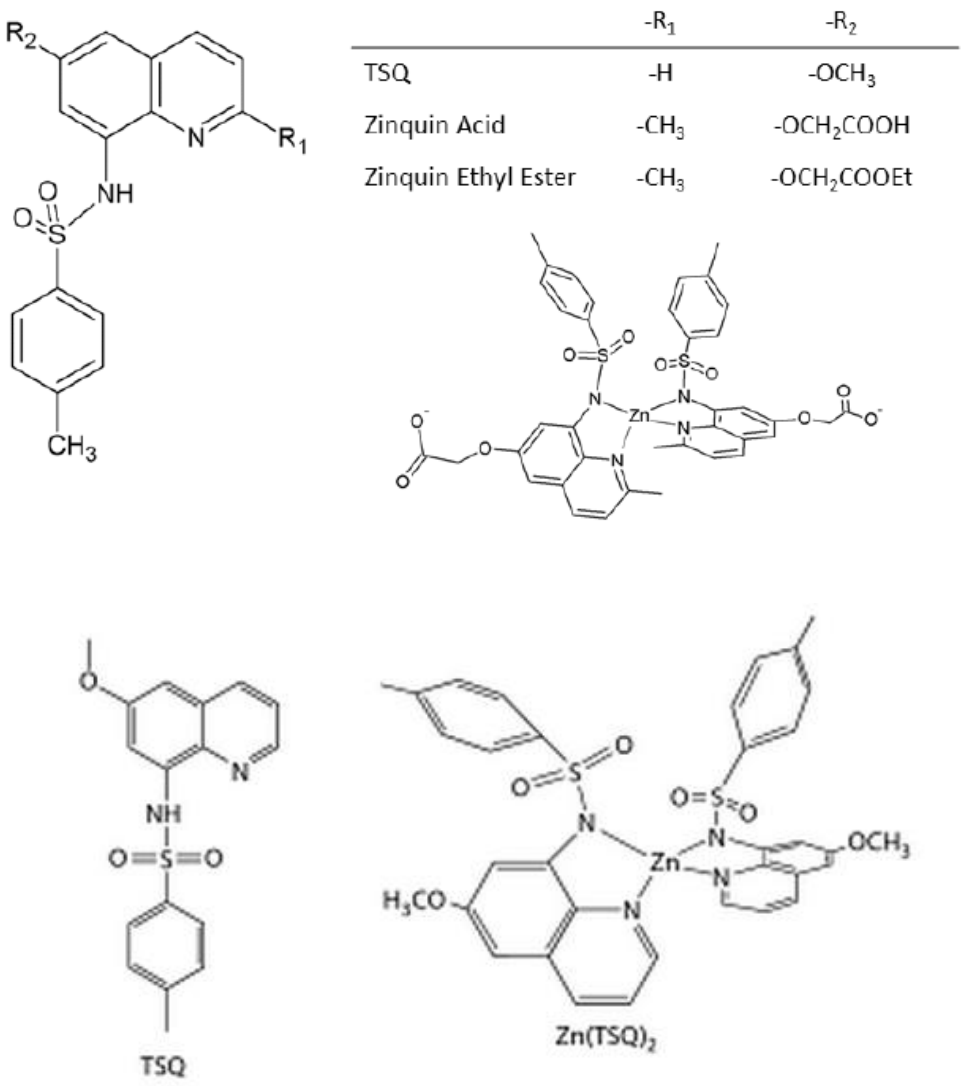

Figure 1.3: Chemical structures of widely used quinoline based zinc sensors. The crystal structures of $Zn(ZQ)_2$ and $Zn(TSQ)_2$.[1]

Using fluorescence microscopy, cells stained with TSQ generally show a punctate staining pattern that was originally interpreted as revealing localized, high concentrations of Zn^{2+} in the cellular environment.[1]

Another zinc sensor that emerged from the same quinoline sulfonamide based family is (2-methyl-8-p-toluenesulfonamido-6-quinolyloxy)acetate, or Zinquin (ZQ), which largely replaced TSQ as a Zn^{2+} sensor. Zinquin was introduced to overcome perceived shortcoming of TSQ. Since both TSQ and $Zn(TSQ)_2$ are chargeless, cellular efflux of the sensor or the zinc-sensor complex may occur. To avoid this, an ethyl ester moiety was substituted at the 6 position (R_2) of the quinoline ring (see Figure 1.3). This chargeless molecule passively enters into the cells, and once inside, is hydrolyzed by intracellular esterases to a negatively charged carboxylic acid, possibly trapping it into the cell. Additionally, a modification was done by adding a methyl group at the 2 position of the quinoline ring (Figure 1.3). The methyl group sterically hinders the formation of square planar and octahedral complexes and favors the tetrahedral complex in a 2:1 binding. This modification also enhances Zinquin's affinity for Zn^{2+} in comparison with TSQ.

1.5. Small molecule ligands of interest

Fluorescent zinc sensors have been widely used as microscopic tools to image Zn^{2+}on a cellular level. Experiments in the Petering laboratory have established that TSQ and Zinquin do not form Zn-Ligand complexes when they enter cells. Instead, they form adducts with Zn-proteins and image a fraction of the Zn-proteome.[1,38,39] It is thought that adduct formation occurs either because Zn^{2+} binding sites of Zn-proteins are unsaturated with ligands or the Zn-coordination sphere can be expanded.

$$\text{TSQ/ZQ} + \text{Zn-proteome} \leftrightarrows \text{TSQ/ZQ-Zn-proteome} \qquad (1.7)$$

Since TSQ and Zinquin bind to many Zn-proteins, it is hypothesized that other metal binding ligands, both synthetic and natural, may also bind to the Zn-proteome.

The purpose of this dissertation research was to expand on the initial hypothesis of the adduct forming property of the Zn-proteome to determine the capacity of the Zn-proteome to form adducts with a variety of synthetic ligands and ligands native to the mammalian cell. Biologically active 1,10-phenanthroline (Phen), related molecules (See Figure 1.4), some natural biomolecules, and other synthetic bidentate ligands were investigated for their ability to bind to Zn-proteome. 1,10-phenanthroline (Phen) is a bidentate ligand, that has long been studied in biological systems, most recently as a copper complex with potential antitumor activity.[40] In this dissertation study, it was observed that Phen and some other metal binding multidentate ligands such as glutathione , were able to displace TSQ from the adduct of TSQ-Zn-proteome and form a non-fluorescent adduct species (Figure 1.4).

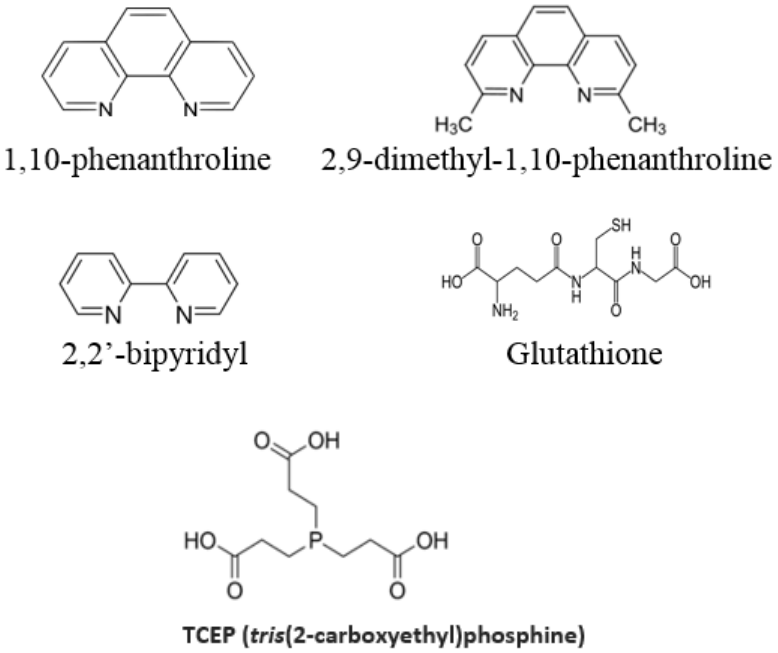

Figure 1.4: Some small molecule ligands. The chemical structures of 1,10-phenanthroline, and some other commonly used ligands in biomedical research.

In summary, the Zn^{2+} trafficking is an intriguing field in biochemistry and the fluorescent biosensors have been particulary employed as a necessary tool to image Zn^{2+} in cellular proteins. The current research demonstrates the capacity of multiple small molecule multidentate ligands to form adducts with the Zn-proteome.

Project goals

1. To determine whether small molecule multidentate ligands form adducts with the Zn-proteome.
2. To Identify and investigate whether these small molecule ligands are capable of binding a model Zn-protein, alcohol dehydrogenase.

2. Methods

2.1. *Chemicals*

All chemicals for experiments were purchased from Sigma-Aldrich, Fischer Scientific and Worthington Chemicals, unless noted. TSQ (AnaSpec) was solubilized in DMSO, at stock concentrations of 5 mM, 2mM and 1 mM. Prepared stock solutions of TSQ were kept in the dark until needed. Stock concentrations were diluted with Tris-HCl for later use in experiments. The TSQ solutions was used within two weeks of preparation.

Model protein alcohol Dehydrogenase was obtained from Worthington Biochemical. Approximately, 10-15 mg of lyophilized powder were dissolved in degassed 20 mM Tris-HCl solution maintained at pH 7.4, and was kept in 4°C. Protein samples were used within two weeks after preparation.

1,10-phenanthroline was purchased from Acros Organic and was solubilized in DMSO to make a stock solution. The stock solution was always diluted in 20 mM Tris-Cl, pH 7.4 before using in any reactions.

TCEP (tris(2-carboxyethyl)phosphine) was acquired from Hampton Research. Initially, 68 mM stock solution was prepared in 20 mM Tris-Cl, pH 7.4. The solution was stored in 4°C, diluted and used when it was needed.

2.2. *Cell Culture*

The LLC-PK_1 cell line (transformed kidney epithelial cells from *Sus Scrofa* (pig)) was purchased from American Tissue Culture Company (ATCC CL101). Frozen LLC-PK_1 cells were thawed after

removal from the very low temperature of -80°C. The cells were transferred into 15 mL media (Sigma) contained in culture flasks, and incubated at 37°C in the presence of 5-6 % CO_2. The LLC-PK_1 (Sus Scofa (pig)) kidney cell lines were grown in Media M199/HEPES and that was supplemented with 4% fetal calf serum (FCS). Before the cells were grown, the media was additionally supplemented with 50 mg/L of antibiotics, both penicillin and streptomycin. The media was exchanged regularly after 48-72 hours with fresh, complete media. When the cells reach confluence, the cells were detached with the treatment of 1 mL trypsin/EDTA solution, centrifuged at 680 x g for 4 minutes and resuspended to complete media around the concentration of 1-2x10^5 cells/mL and then divided among 100 cm^2 cell culture plates.

2.2.1. *Viability Assay*

In order to find the toxicity of the chemicals that were used in the experiments, a cell viability test was carried out. The toxicity was assessed in dose and time dependent fashion. 1 mL media M199 containing a suspension of LLC-PK_1 cells was grown in a 24 well plate. The plates were maintained in an incubator for 1-2 days before the experiment was run to check the cytotoxicity of the ligands.

The viability test utilized the MTT assay that involves the conversion of the tetrazolium salt 3-(4,5-dimethyl-2-thiazole)-2,5-diphenyl-2H-tetrazolium, bromide (MTT) to formazan.[41] The conversion of MTT to formazan producing formazan salt depends on the mitochondrial electron pathway, which is necessary for ATP production. MTT was prepared in saline solution at 5 mM and syringe filtered to sterilize the solution and remove the insoluble particles. MTT was added to cells grown on 24 well plates and incubated for 2-3 hours at 37°C. Media was removed from

the plates and 1 mL of acidified (0.4 N HCl) isopropanol was added to each well to dissolve the dark blue formazan crystals. The absorbance of the resultant solution at 570 nm and 630 nm was measured and the difference of A_{570}-A_{630} was recorded and calculated as a relative measure of viability when normalized to zero exposure samples.

2.2.2. *Spectrophotometry of Whole Cells*

In 100 cm^2 cell plates, cells were grown and kept in an incubator until they reached confluency. When the cells were ready to harvest, the media M199 was removed and the plates were washed 3 times with cold choline phosphate buffered saline (4.7 g NaH_2PO_4, 1.0 g Na_2HPO_4, 32.2 g NaCl, and 25.0 g Choline Chloride in 3.8 L ddH_2O). One mL of Dulbecco's phosphate buffered saline (4.7 g NaH_2PO_4, 1.0 g Na_2HPO_4, 32.2 g NaCl, and 25.0 g Choline Chloride in 3.8 L ddH_2O) was added and cells were gently scraped using a rubber scraper. The cells were loosened from their clumped state into suspension by pipetting up and down two times using a plastic one mL pipette. When the suspensions from various plates were ready, they were pooled, transferred into a 50 mL centrifuge tube, and spun down at 680 x g for 4 minutes. The cell pellet was resuspended in a fluorescence cuvette with a 1 mL aliquot of PBS.

In the spectrofluorometer the background emission was recorded. The fluorescence of the whole cells was recorded before and after exposure to TSQ, with the latter continuing for 30-60 times. The cells were mixed periodically to maintain a homogeneous suspension of the cells. Additional spectra were recorded until the fluorescence reached a maximum stable level. The initial background fluorescence spectrum of the cell population was subtracted from subsequent spectra.

2.2.3. *Cell Lysate Preparation*

Sonication was used to open the outer membrane of the cells and also to disrupt the internal organelle membranes. Cells were collected via centrifugation at 680 x g for 4 minutes at room temperature. The cell pellet was resuspended in one mL of cold ddH2O per 10 plates of cells. The harvested cells (see 2.2.2) in DPBS were then transferred to a plastic cut-off tube and were ready for sonication. Before sonication the flat tip of the sonicator was placed in ice to chill for at least 20 minutes. The cell suspension was sonicated at power 5 for 60 pulses and a total time of 24 seconds. The sonicated cells were transferred to a 15 mL Corex tube until the entire cell suspension was lysed. For experiments resulting in the isolation of the cellular proteome, 1000 units of Benzonase® nuclease (Sigma) and 500 µM phenylmethanesulfonyl fluoride (PMSF) protease inhibitor were added to enhance hydrolysis of nucleotides and suppress degradation of proteins. The sonicates were pooled and spun down in a Sorvall ultracentrifuge 47000 x g for 20-25 minutes in 4°C temperature. The resulting supernatant is called the 'cell lysate'. As needed, the cell lysate was further loaded into a G-75 gel filtration column and separated in a fraction collector to obtain the "proteome" using the chromatographic technique described in the procedure below.

2.3 *Chromatography*

2.3.1. *Sephadex G-75 and G-25 Gel Filtration*

Various types of size exclusion chromatography were employed to separate complex mixtures. For the isolation of zinc proteome, Sephadex G-75 and G-25 gel filtration chromatography beads were purchased from GE Healthcare. Before loading into the column, the beads were soaked in

20 mM Tris-Cl overnight in refrigerator at 4°C, at pH 7.4. The columns were prepared from 0.75 mm round borosilicate glass tubing cut to 90 cm lengths fitted at one end with a plastic stopcock. A small amount of the glass wool was inserted to the bottom of the column. After overnight soaking the hydrated G-75 beads were degassed using aspiration in a sidearm flask for 30 minutes before loading into the column. Approximately, 5 mL of the Sephadex G-75 slurry were then poured slowly and carefully until the column was homogeneously packed, leaving some room on the top of the column for approximately 10 mL of solvent buffer. A one liter round bottomed reservoir flask was attached to the top of the column and filled with Tris-Cl buffer; and the column was allowed to elute by gravity. The column was washed with at least 100 mL of buffer before use. Unless otherwise noted, columns were eluted using degassed 20 mM Tris-Cl pH 7.4. When the columns lost their seal and dried out or when the flow rate exceeded 1 drop every 20 seconds, the Sephadex beads were replaced.

Typically fractionation involved collecting 25-50 drop fractions, corresponding to 1.0-2.0 mL. For Sephadex G-75 separation, 50 one-mL fractions were collected with a total fractionation time of 1.5-2.5 hours. Usually, the first 8 fractions represent the void volume, fractions 10-20 contained the high molecular weight (HMW) proteome, larger than 10 kD in molecular weight.

In Sephadex G-25 size exclusion chromatographic separation, fractions 7-13 included the high molecular weight (HMW) proteome.

2.3.2. *HPLC-DEAE Ion Exchange Chromatography*

Macro-prep DEAE ion exchange cartridges (5 mL) were purchased from Bio-Rad. The ion exchange matrix was generated by elution with 5 column volumes of 5 mM Tris-Cl, pH 8.0

containing 1 M NaCl followed by an additional 5 column volumes with 5 mM Tris-Cl pH 8.0 containing no salt.

Protein solution was loaded into the column using a peristaltic pump, set with the flow rate of 1 mL/min, in a loop, meaning the flow through from the column was directed back into the protein sample feeding the column. The cycle was performed for 30 minutes, to ensure maximal sample load onto the DEAE matrix. Elution of the column was performed using a step wise gradient. In brief, a 10 mL upside down syringe, without the plunger, was connected to the peristaltic pump using Tygon tubing, which then fed the column.

Using a constant flow rate of 1 mL/min, 7 mL of buffer—5 mM Tris-Cl pH 8.0—was loaded into the syringe and then allowed to flow until empty. The syringe was then replenished with 7 mL of new buffer containing a higher salt concentration. A typical stepwise gradient was conducted using 50 mM NaCl increments from 0-500 mM NaCl. 1 mL fractions were collected from the column and the conductivity was determined using a Radiometer CDM 3 conductivity meter.

2.4. *Analytical Measurement and Determination*

2.4.1. *Fluorescence spectrophotometry*

All fluorescence spectroscopy experiments were carried out using a Hitachi F-4500 spectrofluorimeter in fluorescence acquisition mode. For measuring fluorescence emission spectra the spectro-fluorometer settings were as follows. Zn-proteins were imaged using an established fluorophore TSQ. Its excitation wavelength was 370 nm and emission spectra were acquired between 400-600 nm. Instrument parameters were set to a 10 nm aperture and a 5 nm

aperture on the photomultiplier emission tube with the lamp set at 950 V. Data acquisition was carried out in scanning mode at 240 or 1200 nm per second.

2.4.2. *Ultraviolet-Visible spectroscopy*

A Beckman Coulter, DU® 640 spectrophotometer was used to measure the absorption spectra of chromophores in samples or absorbances at their $\lambda_{max.}$ One-cm quartz or plastic cuvettes were used for UV (200-400 nm) and visible (400-600 nm) measurements, respectively. The Beer-Lambert Law was applied to determine the concentration of species based on their measured absorbances.

$A = \varepsilon bc$

in which,

A= absorbance

ε= Extinction Coefficient (M^{-1} Cm^{-1})

c= Concentration (M)

2.4.3. *Zinc determination using Flame Atomic Absorption Spectroscopy (AAS)*

In most experiments, the metal concentrations were measured using flame atomic absorption spectroscopy (AAS). The GBC AAS instrument was set up with an acetylene torch using an 80:20 mix of compressed air and acetylene. A zinc element lamp was used for zinc concentration measurements and a deuterium lamp provided for background correction. Data acquisition was performed in running mode and was calibrated prior to each run using standards of 0.5 ppm, 1.0 ppm and 2.0 ppm Zn^{2+} which corresponds to 7.7 uM, 15.4 uM and 30.8 uM Zn^{2+}

respectively. When, the concentration of Zn^{2+} was higher than 30 uM, the solution was diluted and the Zn^{2+} concentration was remeasured.

2.4.4. *Protein Determination via DC Protein Assay*

The protein concentration of a given sample was measured using the DC Protein Assay kit from Bio-Rad Scientific. This is a colorimetric assay based on the reaction of protein with an alkaline copper tartrate solution followed by the Folin reagent, similar to the Lowry assay.[42] Solutions containing 0.085, 0.17, 0.34, 0.68, 1.36 mg/mL BSA were used as protein standards. In most cases 25 uL of sample were mixed with 125 uL of Reagent A (copper solution) and immediately vortexed for 5 seconds. One mL of the Reagent B (Folin solution) was then added and the solution was again vortexed for 5 seconds. After 15 minutes the absorbance at 750 nm was recorded. The unknown protein concentrations (mg/mL) in the samples were determined using Bovine serum albumin standard curve.

2.5. *Poly Acrylamide Gel Electrophoresis (PAGE)*

All gel electrophoretic methods were performed using Novex® NuPAGE® precast gels in conjunction with the XCell SureLock™ Mini-Cell electrophoresis chamber available from Invitrogen.

2.5.1. *Native Sodium Dodecyl Sulfate (NSDS) PAGE*

NSDS run buffer samples were chilled on ice for 30-40 minutes at 4°C before the protein sample preparation. The NSDS run buffer was composed of 50 mM Tris, 50 mM MOPS, 0.0375% SDS, pH 7.6.[43] The NuPAGE® 12% Bis-Tris pre-cast gels were assembled in the electrophoresis chamber and a pre-run of the gel was carried out at 150 V for at least 30 minutes using ddH_2O as the run buffer. Protein samples were mixed with 4X sample buffer (100 mM Tris HCl, 150 mM Tris Base, 10% glycerol, 0.0185 % Coomassie G-250, 0.000625% Phenol Red, pH 8.5) and loaded into pre-run gels. The electrophoresis chamber was filled with the pre chilled NSDS run buffer. The electrophoresis was carried out at 150 V, at 4^{o}C for 85-90 minutes until the dye front migrated 60 mm. Gels were stained with TSQ, ligands, and Coomassie Blue as described.

2.6. *Gel staining technique*

2.6.1. *TSQ staining and imaging of gels*

Gel staining experiments were performed at the Children's Environmental Health Sciences Core Center Laboratory in the School of Freshwater Sciences. Electrophoresis of the protein samples was carried out using the NSDS-PAGE technique as described in section 2.5.1. The plastic cassettes of the gel were separated and were gently washed with 100 mL ddH_2O two times. The gel was then carefully transferred for imaging. The gel was transferred into a UVP EpiChemi II Darkroom UV transilluminator gel box set at the long UV wavelength (approximately 365 nm) setting. Images of the gel were taken using a digital camera with a 470 nm emission filter and processed using LabWorks software version 4.5. Typical exposure times for fluorescent images were between 3-10 seconds.

First a background picture was taken to rule out auto fluorescent protein bands. After background imaging, the gel was transferred in a shallow disk containing 50 mL of 25 uM TSQ solution in ddH_2O. The gel was soaked and kept in a rotatory shaker for about 40 minutes. Subsequently the gel was washed with ddH_2O two times for 5 minutes. A picture of the stained gel was captured using the Gel Documentation System as noted before. Next, the gel was treated with 50 mL 250 uM 1,10-phenanthroline solution in ddH_2O for 30 minutes and imaging was done to see the effect of the ligand on TSQ stained gels.

2.6.2. *Coomassie R-250 protein band staining*

After gels were removed from their casings, they were placed in a 100 mL fixing solution, containing 40% methanol and 10% acetic acid, microwaved for 45 seconds, and put on an orbital shaker for 30-35 minutes. The gel was incubated in the fixing solution for 1 hr with gentle agitation. This process was followed twice. The fixing solution was decanted and 50 mL of the staining solution (30 % methanol, 10 % acetic acid, 0.002% Coomassie R-250) added. Gels were microwaved for 45 seconds and placed on the orbital shaker for overnight. The gels were destained by incubating in 100 mL of microwaved 8% acetic acid and agitating for 45 minutes. The destaining solution was replaced and the gel was allowed to destain overnight on a shaker.

3. Results

Chapter-1 Cellular Chemistry of 1,10-Phenanthroline

3.1. *Fluorescence Spectroscopy of $Zn(TSQ)_2$*

Zn^{2+} imaging is important in the cell to understand the biochemistry of zinc. TSQ is a bidentate Zn-imaging agent (Figure 3.1). Originally, it was thought that TSQ imaged cellular Zn^{2+}.[44] However, it has been shown that TSQ actually binds to Zn-proteome not free Zn^{2+}.[1]

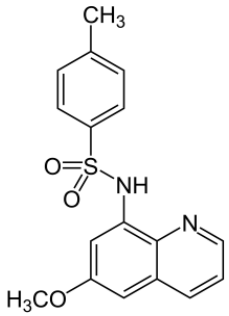

Figure 3.1. 6-Methoxy-(8-p-toluenesulfonamido)quinoline, TSQ

Since TSQ binds to about 15-20% of proteomic - bound Zn^{2+}, it was hypothesized that it could serve as an indicator of the formation of the adducts with Zn-proteome that involve either endogenous or exogenous Zn^{2+} binding ligands (L).

$$\text{TSQ-Zn-proteome} + \text{L} \leftrightarrows \text{L-Zn-proteome} + \text{TSQ} \qquad (3.1)$$

Whereas TSQ-Zn-proteome is fluorescent, L-TSQ-proteome is not; so the loss of fluorescence decay reaction would signal the presence of L-Zn-proteome. We used 1,10-phenanthroline as the ligand to test the hypothesis.

Before investigating reaction 3.1, control experiments were carried out to demonstrate the appearance of fluorescence upon reaction of Zn^{2+} with TSQ. One mL 10 uM of TSQ was titrated with increasing concentration of Zn^{2+} and over the time the fluorescence intensity change was monitored. The spectral data were plotted in Figure 3.2 and demonstrated the formation of $Zn(TSQ)_2$, with a spectral wavelength maximum of 490 nm.

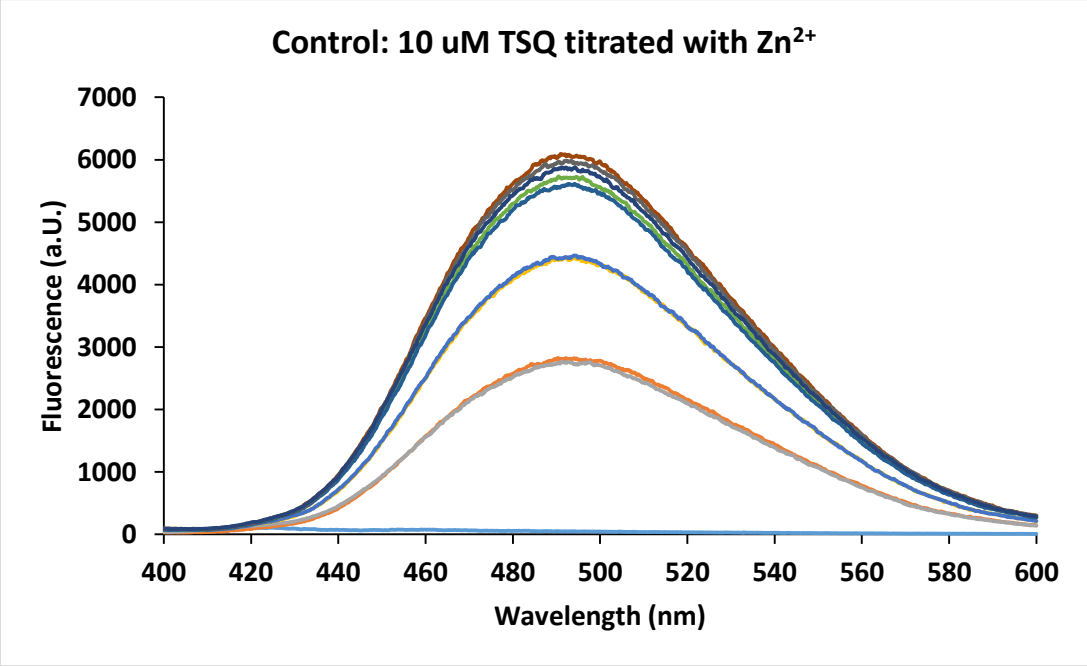

Figure 3.2. Fluorescence spectra of TSQ with Zn^{2+} solution. 10 uM of TSQ in 1 mL of 20 mM Tris-Cl buffer pH 7.4 was titrated with Zn^{2+}. Using an excitation wavelength of 370 nm, the fluorescence emission was recorded from 400-600 using a Hitachi F4500 Fluorescence Spectrofluorometer.

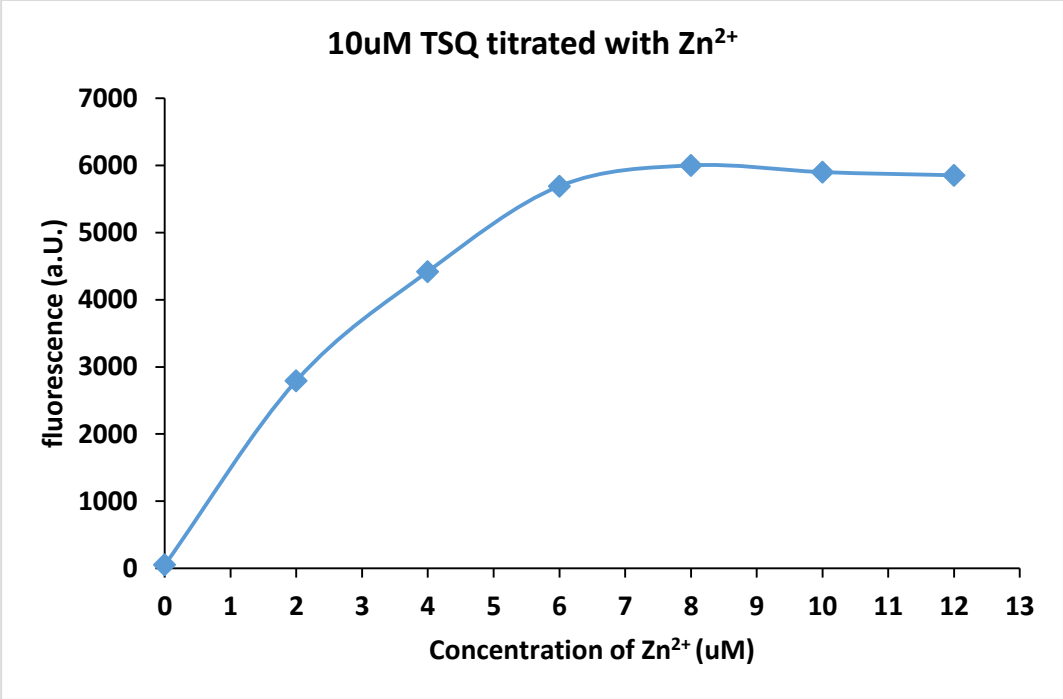

Figure 3.3. Graph of the Concentration of Zn^{2+} vs. Fluorescence intensity at 490 nm. The graph confirms the reaction between TSQ and Zn^{2+} to make a 1:2 complex of $Zn(TSQ)_2$.

$$Zn^{2+} + 2TSQ \leftrightarrows Zn(TSQ)_2 \text{ (complex formation at 490 nm)} \quad (3.2)$$

3.1.1. *$Zn(Phen)_2$ complex formation according to the fluorescence data*

After the formation of $Zn(TSQ)_2$ Figure 3.2, the product was titrated with the ligand 1,10-phenanthroline. The following Figure 3.4, shows that 1,10-phenanthroline can compete with TSQ for Zn^{2+} and displace it, resulting in a binary complex formation of $Zn(phen)_2$. During the reaction the diminishing intensity of the spectra remains centered at 494 nm, indicating that $Zn(TSQ)_2$ is converted to a Zn-phenanthroline complex and does not form a Zn(TSQ)(Phen) mixed ligand complex that would emit fluorescence at about 470 nm, which allows to make strong assumption that 1,10-phenanthroline is capable to bind with Zn^{2+} in a 2:1 ratio.

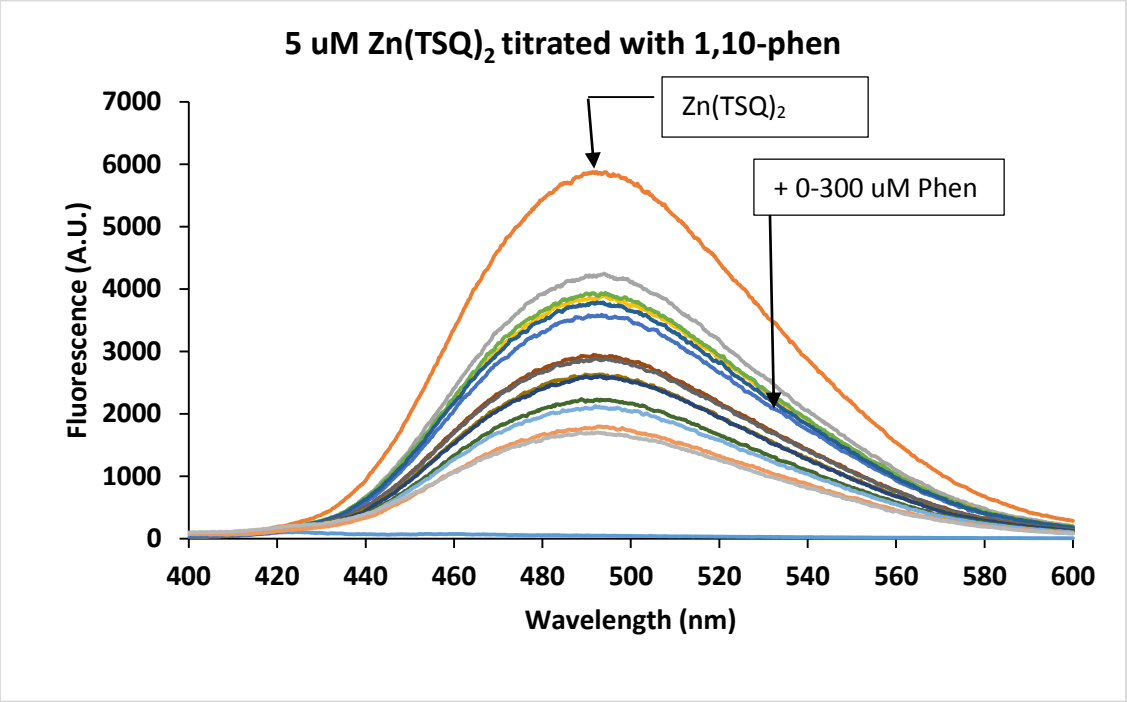

Figure 3.4. $Zn(TSQ)_2$ complex titration with 1,10-phenanthroline. 5 uM $Zn(TSQ)_2$ was titrated with 1,10-phenanthroline (from the stock solution of 10 mM in DMSO and diluted in Tris-Cl buffer pH 7.4). A total 10 uL from 30 mM 1,10-phenanthroline was added that makes 300 uM in concentration.

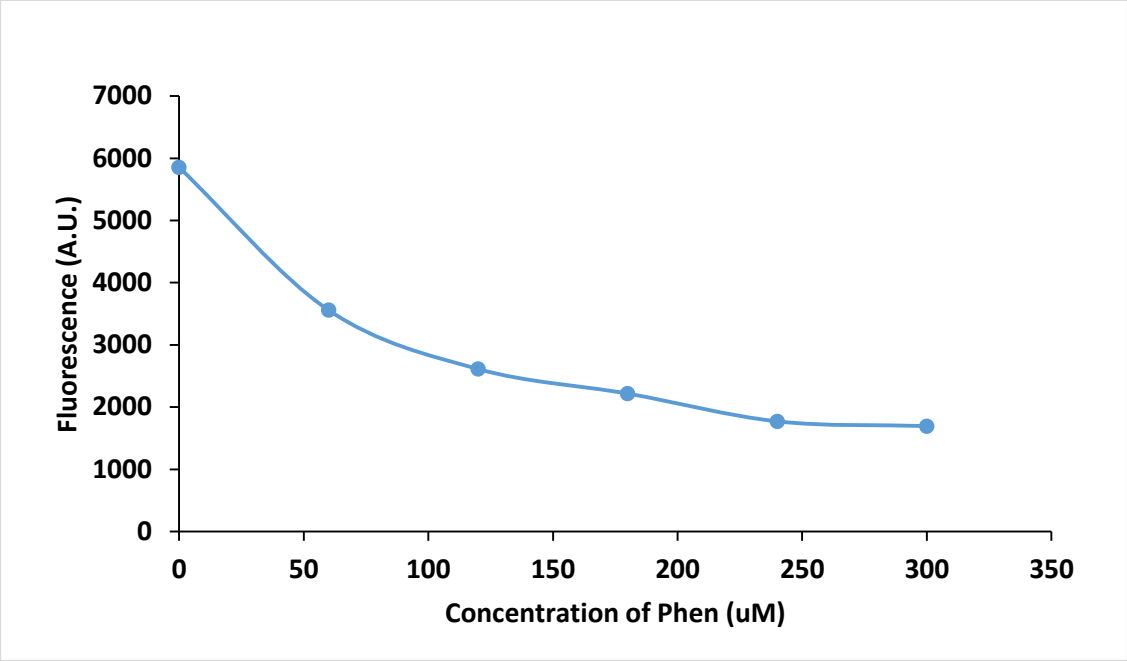

Figure 3.5. The graph of the titration of $Zn(TSQ)_2$ with 1,10-phenanthroline. $Zn(TSQ)_2$ (5 uM) was titrated with 1,10-phenanthroline (from the stock solution of 30 mM in DMSO and diluted in Tris-Cl buffer pH 7.4) up to 300 µM of concentration.

The trend of the titration is shown in Figure 3.5, and it represents that there was a substantial amount of rapid fluorescence decay (Figure 3.5) observed for the first addition of 1,10-phenanthroline. Then for the subsequent additions the reaction continues in a slow progress to replace TSQ.

$$Zn^{2+} + 2TSQ \leftrightarrows Zn(TSQ)_2 \quad (3.3)$$

$$Zn(TSQ)_2 + 2\ phen \leftrightarrows Zn(phen)_2 + TSQ \quad (3.4)$$

3.1.2. *Time dependent reaction of 1,10-phenanthroline with $Zn(TSQ)_2$ complex*

After the study of the concentration dependent titration of the $Zn(TSQ)_2$ complex with Phen a time dependent study was carried out. In order to do that, 1 mL 10 uM TSQ was allowed to react with 5 uM Zn^{2+} and the fluorescence intensity rise was recorded (Figure 3.6) until a maximum stable fluorescence intensity was reached. After the completion of the reaction, 5 uM $Zn(TSQ)_2$ complex was immediately allowed to react with 60 uM Phen and the reaction was monitored over the time of 20 minutes (Figure 3.7). 1,10-Phen very quickly displaces TSQ from the $Zn(TSQ)_2$ complex and a $Zn(Phen)_2$ complex was formed which is indicated by the emission λ_{max} at 490 nm. The initial fluorescence decay was very rapid followed by a slow displacement of TSQ from the $Zn(TSQ)_2$ complex which is an indication of the equilibrium of the reaction of the following reaction.

$$Zn(TSQ)_2 + 2\ Phen \leftrightarrows Zn(Phen)_2 + 2\ TSQ \qquad (3.5)$$

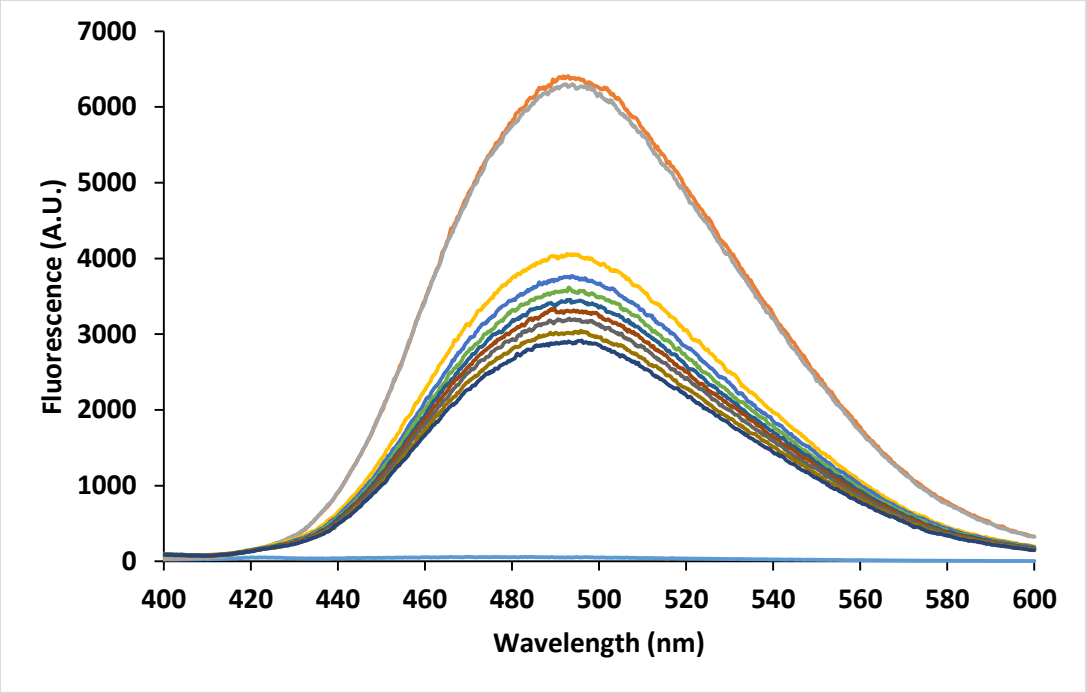

Figure 3.6. Time dependent reaction of 1,10-Phen and Zn(TSQ)$_2$. 5 uM Zn(TSQ)$_2$ was reacted with 60 uM Phen. Over the time continuing 0.5-20 minute fluorescence change was recorded.

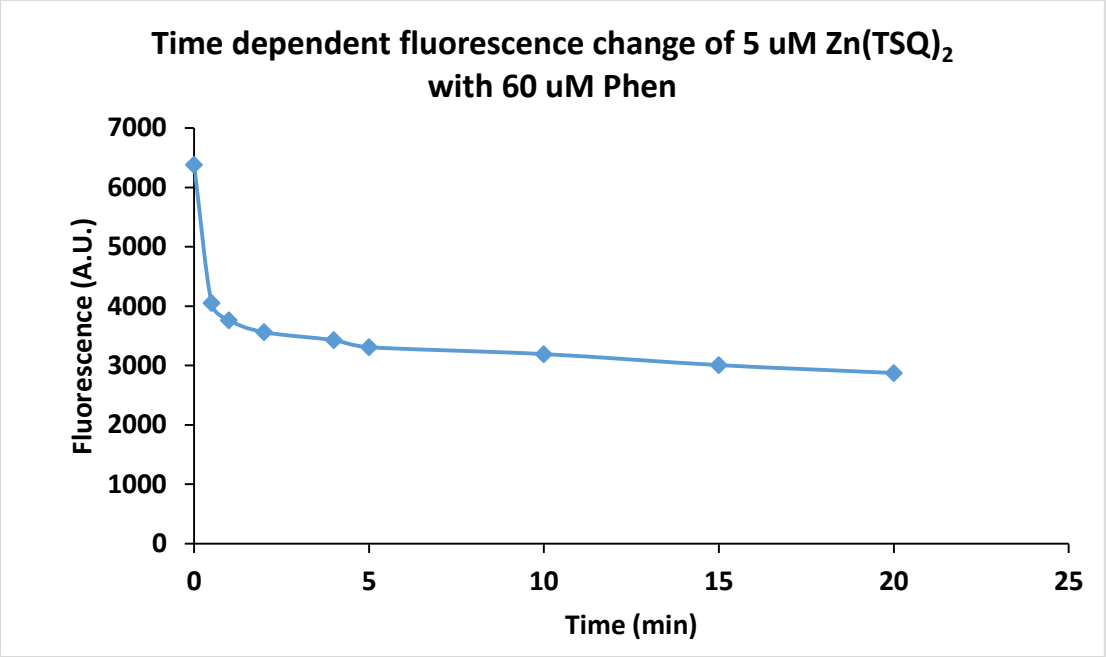

Figure 3.7. Plot of time dependent reaction of 1,10-phenanthroline with $Zn(TSQ)_2$: The fluorescence intensity decay of 5 uM $Zn(TSQ)_2$ after the addition of 60 uM 1,10-phenanthroline.

3.2. *UV data of $Zn(phen)_2$ complex formation*

In accordance with the data of the imaging of $Zn(TSQ)_2$ then the formation of $Zn(phen)_2$, UV-Vis absorbance spectrophotometry was used to come up with a strong conclusion that $Zn(Phen)_2$ complex formation had occurred. During the titration of Phen with Zn^{2+}, UV spectra were obtained in the range of 220-320 nm wavelength. In the Figure 3.8, the data were plotted and a signature spectrum for 1,10-phenanthroline was independently obtained and a spectrum was recorded at 263 nm region in the UV spectrum. Then the titration with Zn^{2+} was followed until 42 uM of total Zn^{2+} (in terms of concentration) addition. It is clear from the data of the Figure 3.8, that 1,10-phenanthroline makes complex formation in 2:1 ratio with Zn^{2+}. The $Zn(Phen)_2$ complex shows UV-absorbance maximum intensity at 270 nm wavelength (Figure 3.9). This novel idea

from the signature proof of the $Zn(phen)_2$ complex formation using UV-Vis spectroscopy further lead to pursue on the rest of the experiments in the cellular environments.

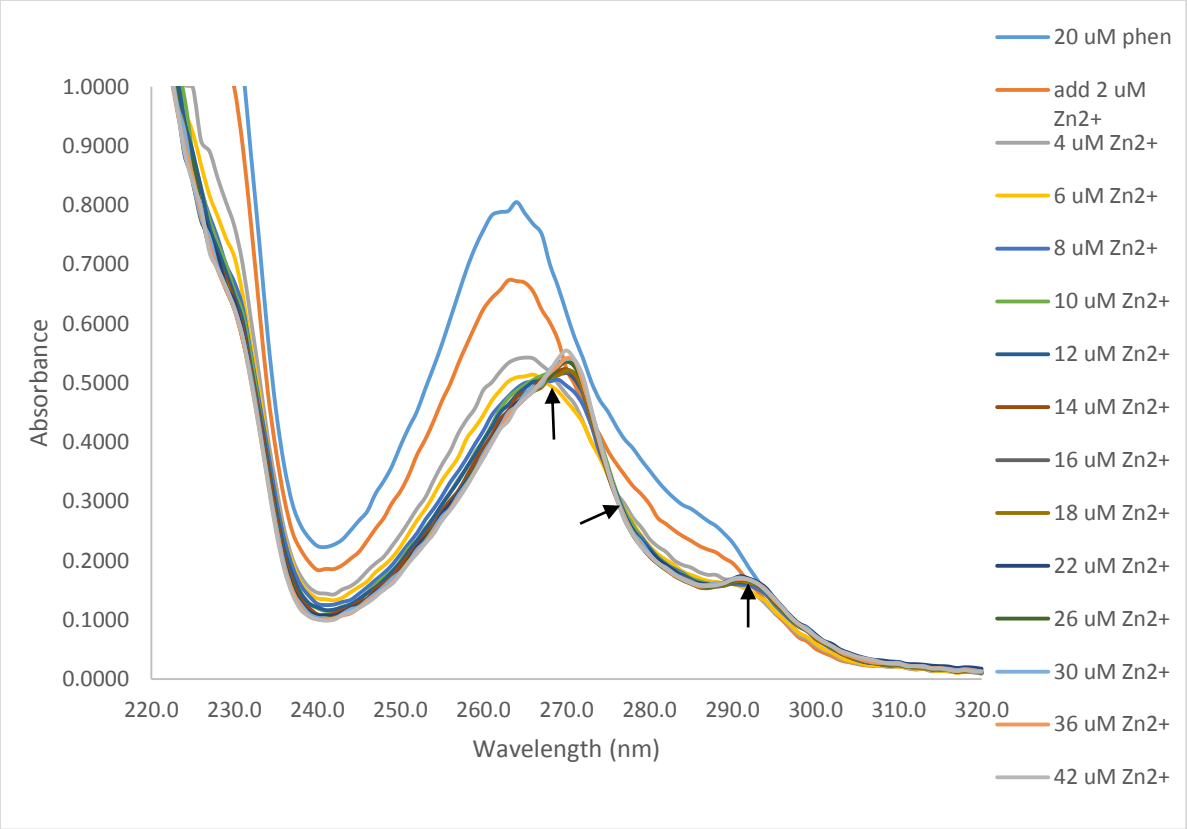

Figure 3.8. UV-Vis Spectroscopy of titration of Phen with Zn^{2+}. 20 uM of 1,10-phenanthroline was reacted with 0-42 uM of Zn^{2+} in 20 mM Tris-Cl, pH 7.4. Absorbance was recorded from 220-320 nm using a Beckman DU-640 spectrometer. Arrows point to isosbectic points.

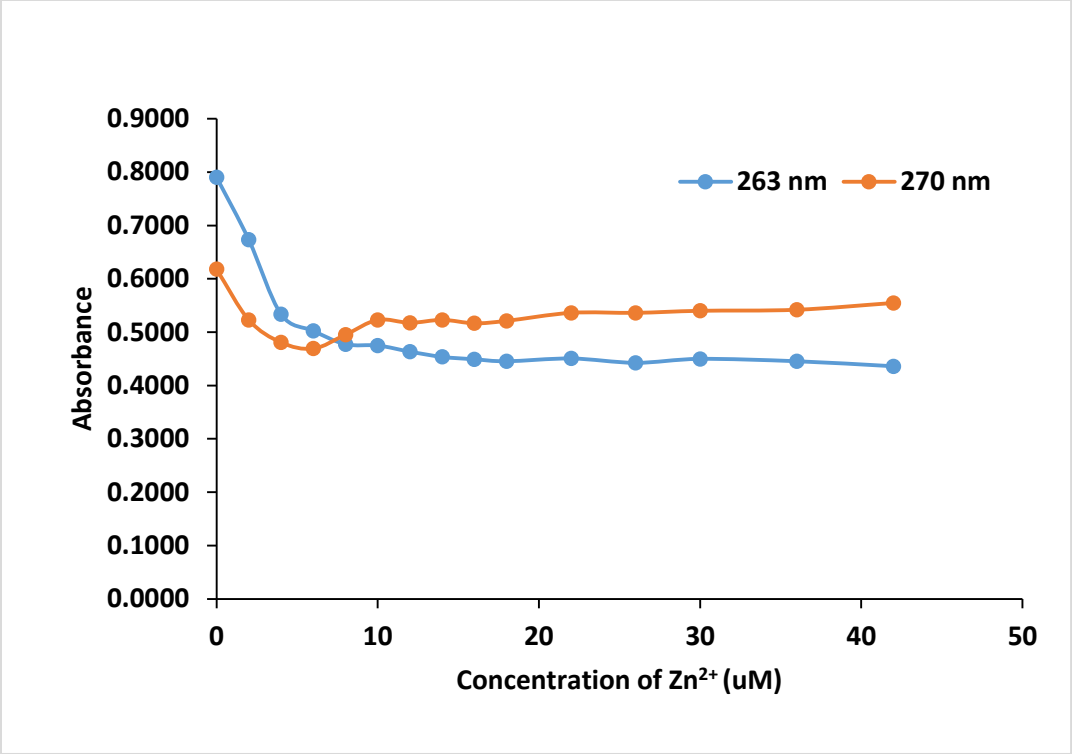

Figure 3.9. The UV-Vis absorbance data of Zn(Phen)$_2$ complex. Zn(phen)$_2$ complex formation at the two prominent isosbectic points (at 263 and 270 nm) were plotted (data from Figure 3.8).

3.3. *Exposing LLC-PK$_1$ whole cells to TSQ in vivo*

To image Zn^{2+} in the living system, LLC-PK$_1$ cells were grown in culture, gently scraped using phosphate buffered saline DPBS and exposed to TSQ in a plastic cuvette. After exposure of 10 uM TSQ in the cuvette, a time dependent increase in the fluorescence was observed and the wavelength of the fluorescence maximum recorded. At 470 nm the intensity of fluorescence was maximum when the cells were directly exposed to TSQ. This gives a clear indication that the Zn-proteins in the whole cells react with TSQ and form ternary adducts, which fluoresce with a wavelength maximum at 470 nm region in the emission wavelength. This can be differentiated readily from the complex formation of Zn(TSQ)$_2$, Figure 3.2, which displays a fluorescence

wavelength maximum at 494 nm according to the fluorescence data. Hence, supporting the data that Zn-proteins in the whole cells can make ternary adduct when it is exposed to the sensor TSQ. Figure 3.10 depicts that the orange line of the highest peak is for the reaction of 1 mL $1X10^7$ LLC-PK_1 whole cells with 10 uM TSQ, the peak was recorded after the maximum reaction was completed with TSQ.

$$\text{Zn-Protein + TSQ} \rightleftarrows \text{TSQ-Zn-Protein (ternary adduct formation at 470 nm)} \quad (3.6)$$

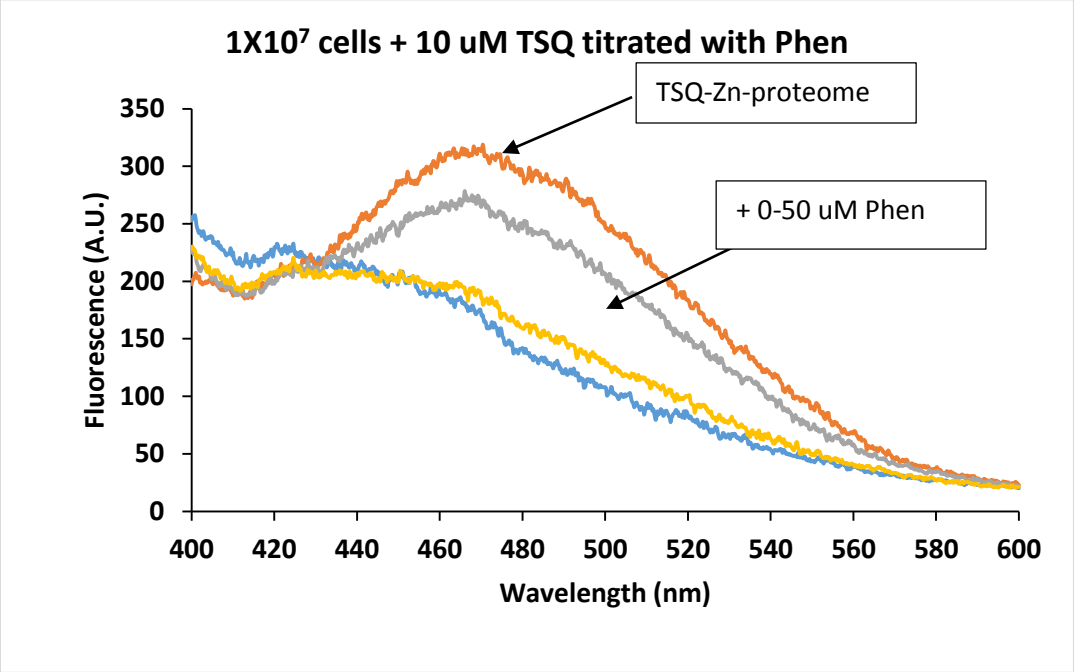

Figure 3.10. Fluorescence spectra of TSQ and 1,10-phen exposed cells. $1X10^7$ cells were suspended in DPBS and reacted with 10 uM TSQ over the time of 20 minutes then the fluorescence spectra were recorded with the stepwise addition of 1,10-phen.

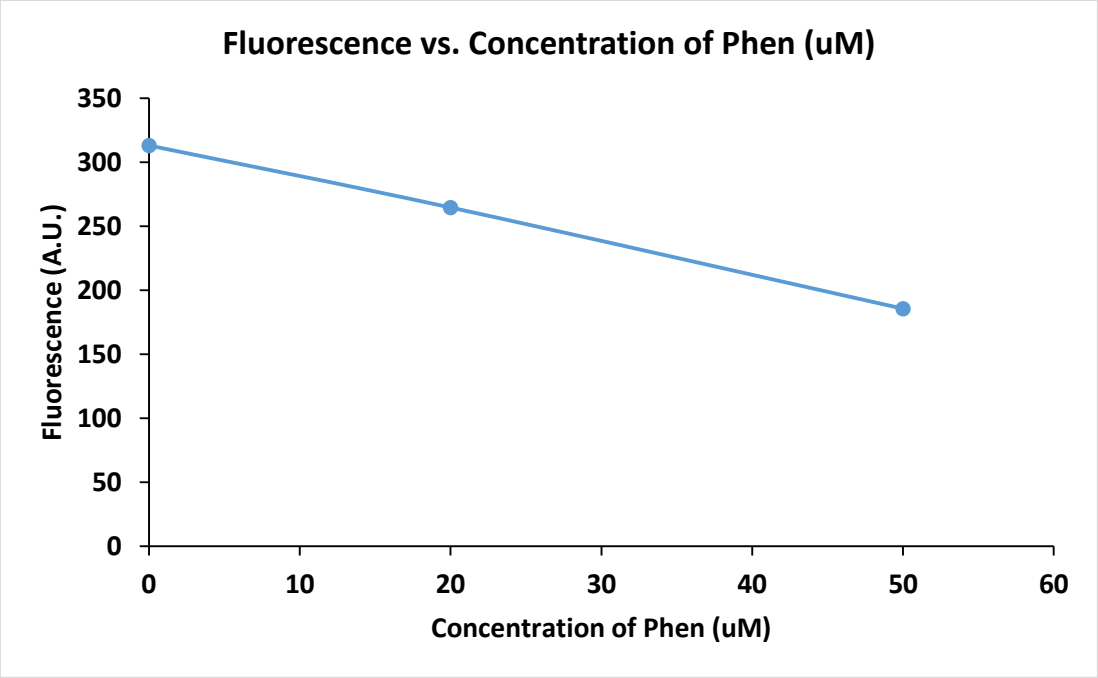

Figure 3.11. Diagram of the concentration of 1,10-phenanthroline vs. Fluorescence. The formation of phen-Zn-protein adduct.

Subsequently, the reaction mixture of LLC-PK_1 whole cells stained with TSQ was titrated up to 50 uM 1,10-phenanthroline. The fluorescence spectrum due to the reaction of TSQ with cells was completely quenched, indicating that ternary adducts of 1,10-phen-Zn-proteins had replaced from those of TSQ-Zn-proteins. The fluorescence data acquisition was continued for 15 minutes though no fluorescence change was observed.

From the data and the results from Figures 3.10 and 3.11, the hypothesis was supported that, 1,10-phenanthroline competes with the fluorophore TSQ in the ternary adduct of TSQ-Zn-proteins and forms 1,10-phen-Zn-proteins. The reaction seems to go to completion indicating that a high a concentration of 1,10-phenanthroline is required to displace all the TSQ towards the completion of the reaction yielding the ternary adduct of 1,10-phen-Zn-proteins.

3.3.1. *Reaction of TSQ and 1,10-phenanthroline with the isolated Zn-proteome from the LLC-PK_1 cell lines*

Zn-proteome is the major source of the fluorescence in cells exposed to TSQ.[1] Further characterization of the reaction of the Zn-proteome with TSQ was performed. The pig kidney cell line LLC-PK_1 was grown, harvested and lysed. Subsequently, it was centrifuged in the Sorvall Ultracentrifuge SS-34 rotor for 20 minutes (at 20,000 ppm and 47,000 X g) and the supernatant passed through the size exclusion Sephadex G-75 column. Fifty fractions, each containing 1 mL were eluted from the Sephadex G-75 column chromatography using degassed 20 mM Tris-Cl buffer pH 7.4. The fractions which absorb at 280 nm in the UV-Vis were pooled and then Zn^{2+} concentration was measured using atomic absorption spectrophotometry (AAS). Based on the Zn^{2+} concentration, 5.7 uM of Zn-proteome was then titrated separately with a concentration up to 20 uM TSQ. The basal fluorescence of the Zn-proteome was recorded and the fluorescence enhancement was observed immediately after the TSQ addition with a blue-shifted emission maxima centered at 470 nm wavelength, data displayed in Figure 3.12.

The mixture of Zn-proteome and TSQ was titrated with 1,10-phenanthroline upto a concentration of 240 uM. A substantial amount of fluorescence quenching was observed with emission maximum wavelength centered at 470 nm. The fluorescence was followed for 130 minutes because the reaction was slow and a gradual loss of fluorescence was observed. Throughout the reaction, the fluorescence emission maximum remained at 470 nm wavelength. The following Figure 3.13 was plotted from the experimental data.

From the above experiment, the results were consistent with the reaction of TSQ-Zn-proteome ternary adduct with 1,10-phen to form phen-Zn-proteome. The exogenous ligand 1,10-phenanthroline competes well with TSQ in a higher concentration and a ternary adduct formation was revealed by showing the quenching of fluorescence of Phen-Zn-proteome.

The reactions could be summarized as follows:

Zn-proteome + TSQ ⇆ TSQ-Zn-proteome (3.7)

TSQ-Zn-proteome + 1,10-phenanthroline ⇆ 1,10-phen-Zn-proteome + TSQ (3.8)

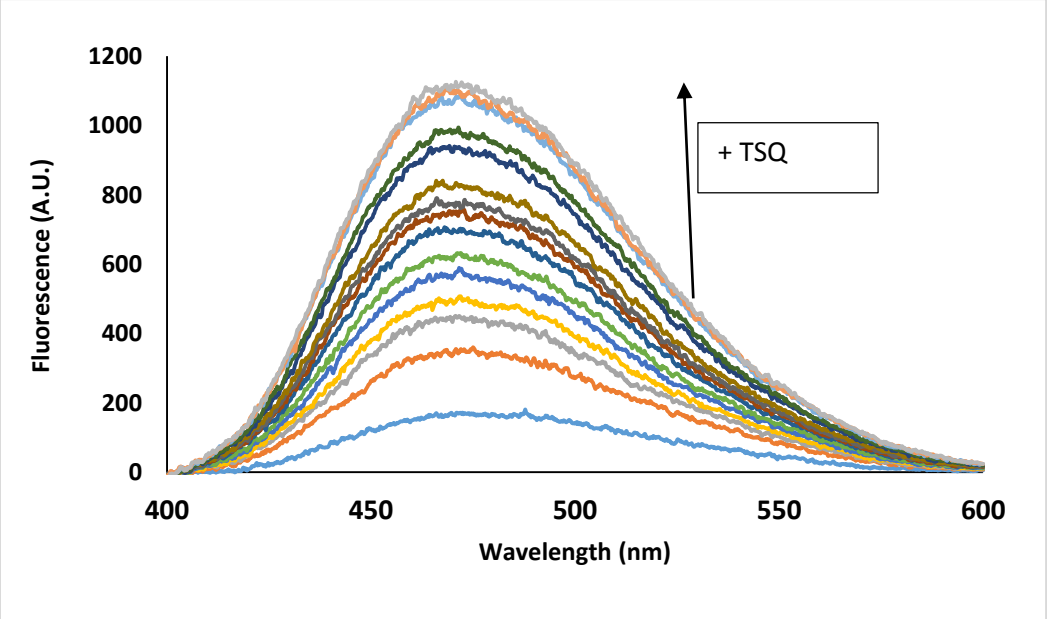

Figure 3.12. Titration of Zn-proteome with TSQ. 5.7 µM Zn-proteome was titrated upto 20 µM TSQ.

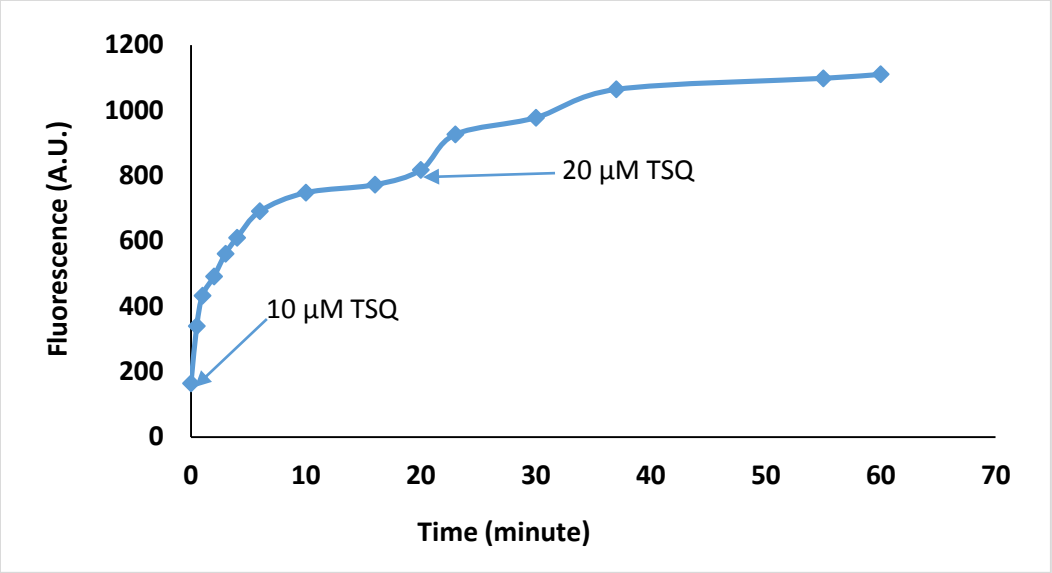

Figure 3.13. Time dependent plot of the addition of TSQ with Zn-proteome. 5.7 µM Zn-proteome was titrated upto 20 µM TSQ and over the time of 60 minutes the fluorscence change was monitored.

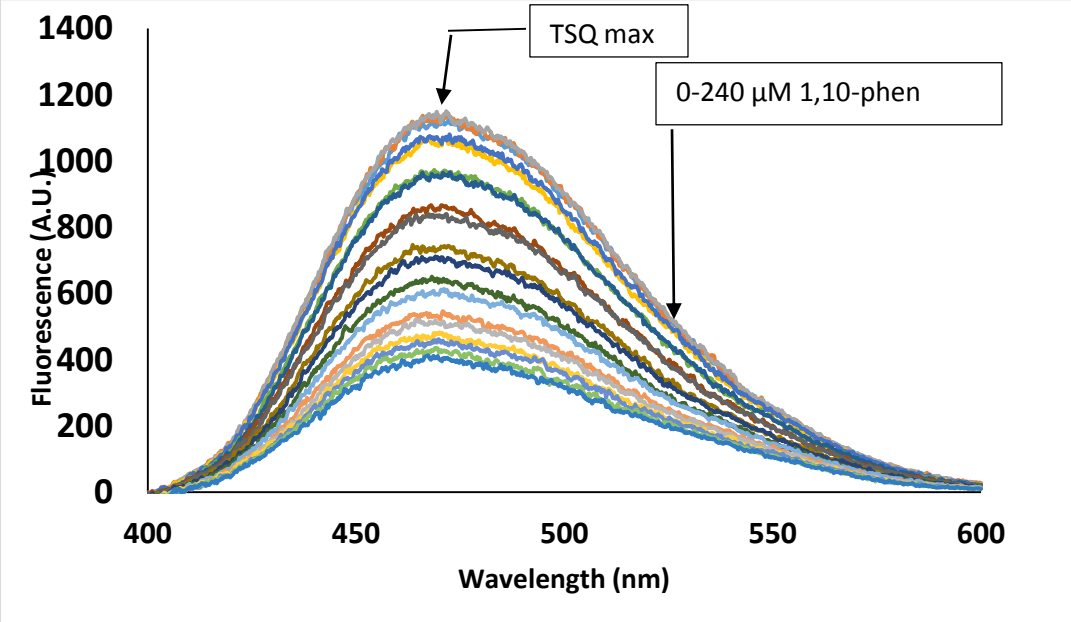

Figure 3.14. Reaction of Zn-proteome with TSQ and 1,10-phenanthroline. 5.7 uM of Zn-proteome was reacted with 20 uM TSQ, then over the time the fluorescence quenching was observed upon stepwise addition of total 240 uM 1,10-phenanthroline.

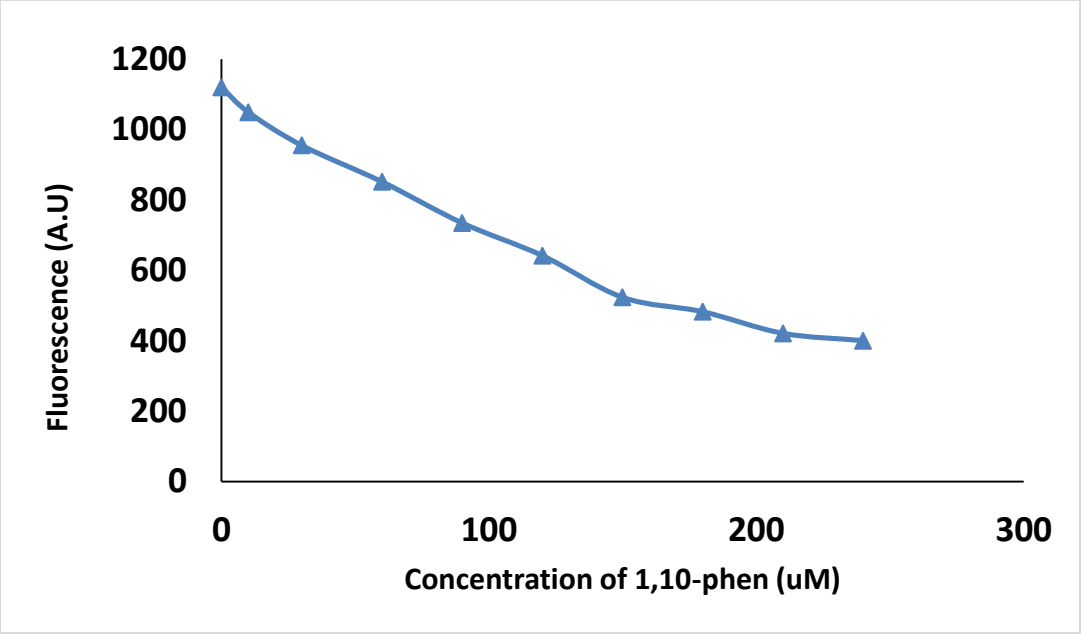

Figure 3.15. The adduct of TSQ-Zn-proteome titration with 1,10-phen. The diagram of concentration dependent titration of 1,10-phenanthroline with TSQ-Zn-proteome adduct.

When the reaction mixture was chromatographed through Sephadex G-75 size exclusion resin, the residual fluorescence centered at 470 nm was retained in the proteome region of the chromatogram that reacted with TSQ and 1,10-phenanthroline respectively, (Figure 3.16). Further, the reaction mixture did not show any fluorescence in the LMW weight fractions, suggesting that there was no production of $Zn(TSQ)_2$, according to Figure 3.17, there was also no sign of Zn^{2+} in the low molecular weight region, indicating that neither TSQ nor phen removed Zn^{2+} from the Zn-proteome. The data of this experiment indicate that 1,10-phenanthroline does not compete for Zn^{2+} in Zn-proteins but only forms adducts.

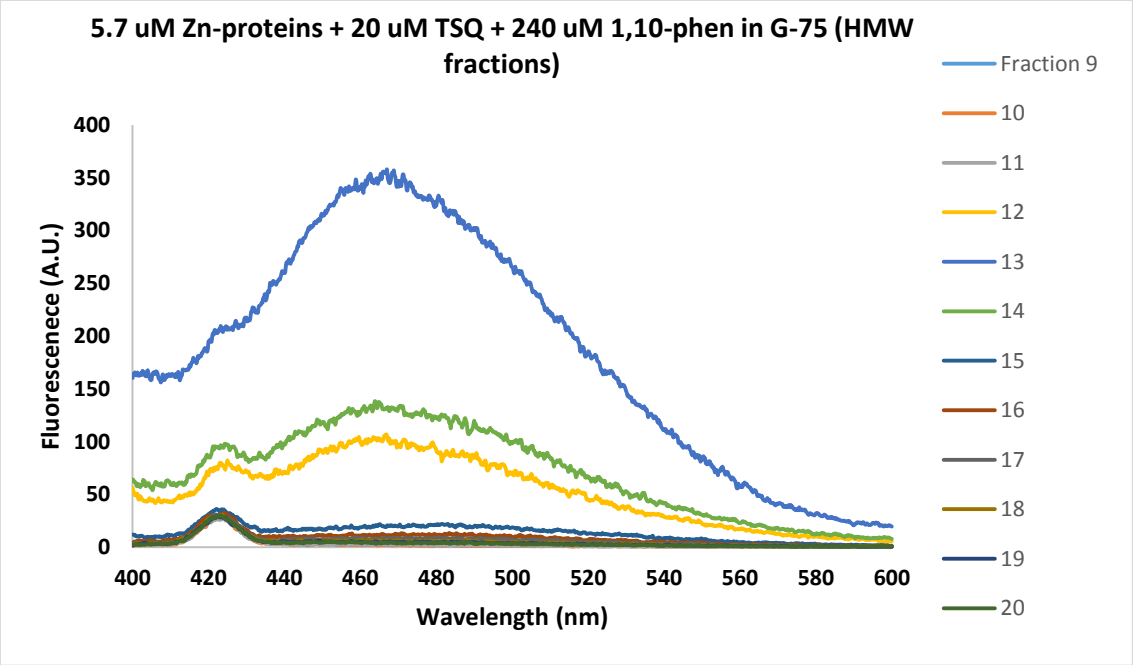

Figure 3.16. Sephadex G-75 column chromatography of the mixture of TSQ-Zn-proteome-phen. High molecular weight fractions from the Sephadex G-75 size exclusion chromatography shows fluorescence centered at 470 nm.

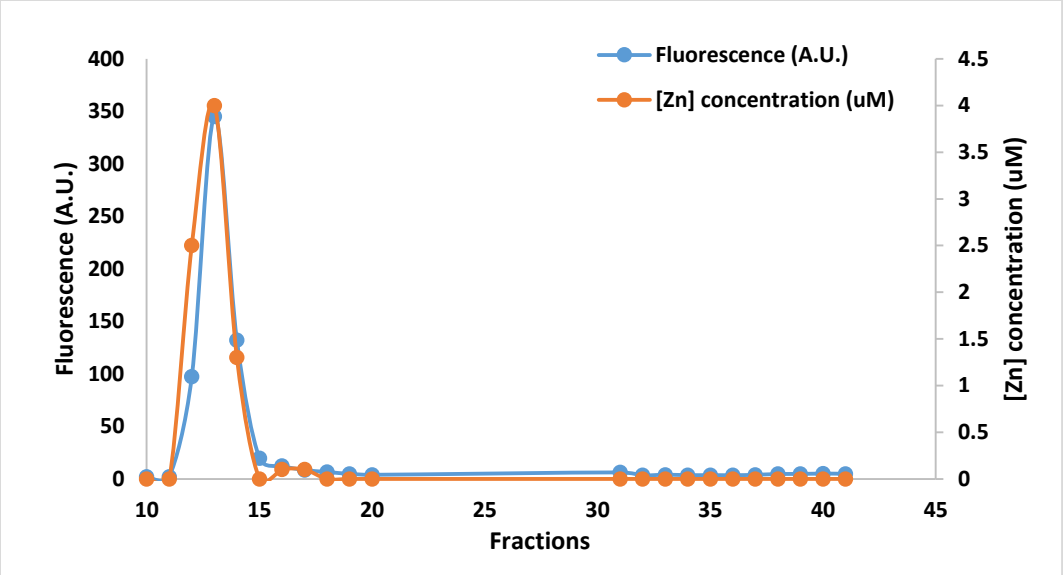

Figure 3.17. Results of Sephadex G-75 chromatography of reaction mixture of TSQ-Zn-proteome and 1,10-phen. The fluorescence and the Zn^{2+} concentrations of the respective fractions of the reaction mixture were plotted according to the data from the fluorescence and AAS.

3.3.2. Time dependent study of the isolated Zn-proteome and 1,10-phenanthroline

After the study of the concentration dependent titration of the isolated Zn-proteome from LLC-PK_1 cells, a time dependent study was carried out. In order to do that, 1 mL 5.7 uM isolated Zn-proteome was first allowed to react and reach almost saturation with 20 uM TSQ in 60 minutes. After the completion of this reaction, 200 uM of 1,10-phenanthroline was added immediately and the reaction was monitored over the time of 55 minutes. 1,10-phenanthroline very quickly displaces about 40% of the TSQ from the adduct of TSQ-Zn-proteome (Figure 3.18). The following Figure 3.19 shows a plot of the data of the time dependent reaction of 1,10-phenanthroline and Zn-proteome. The initial fluorescence quenching is well noticeable by displacing TSQ from the TSQ-Zn-proteome adduct from Figure 3.18. Due to the higher concentration of 1,10-phenanthroline (200 uM) it was an initial 56% of the fluorescence decay, which is consistent with

the concentration dependent titration (see Figure 3.14) of 1,10-phenanthroline with the adduct of TSQ-Zn-proteome. Therefore, the reaction is always maintaining an equilibrium and within the time of 55 minutes after the initial large fluorescence decay there was not any significant change in fluorescence happened.

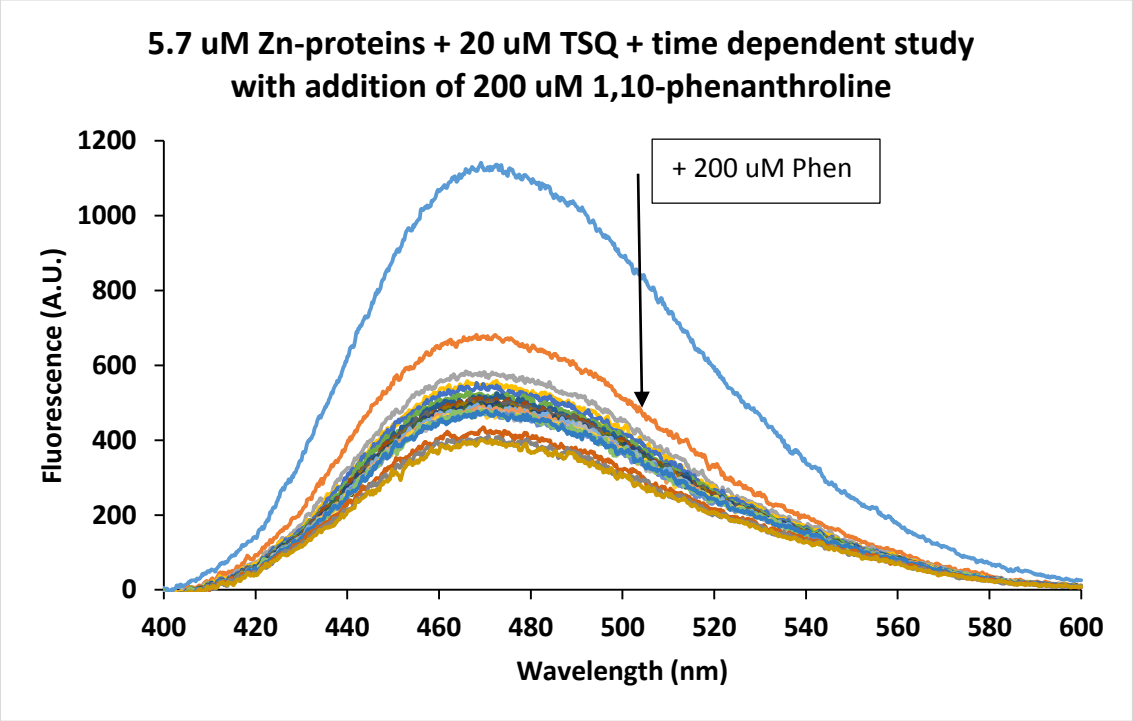

Figure 3.18. Time dependent reaction of 1,10-phenanthroline with TSQ-Zn-proteome. 5.7 uM Zn-proteome was reacted with 20 uM TSQ, then at a time 200 uM of 1,10-phenanthroline was added to monitor the effect of fluorescence change.

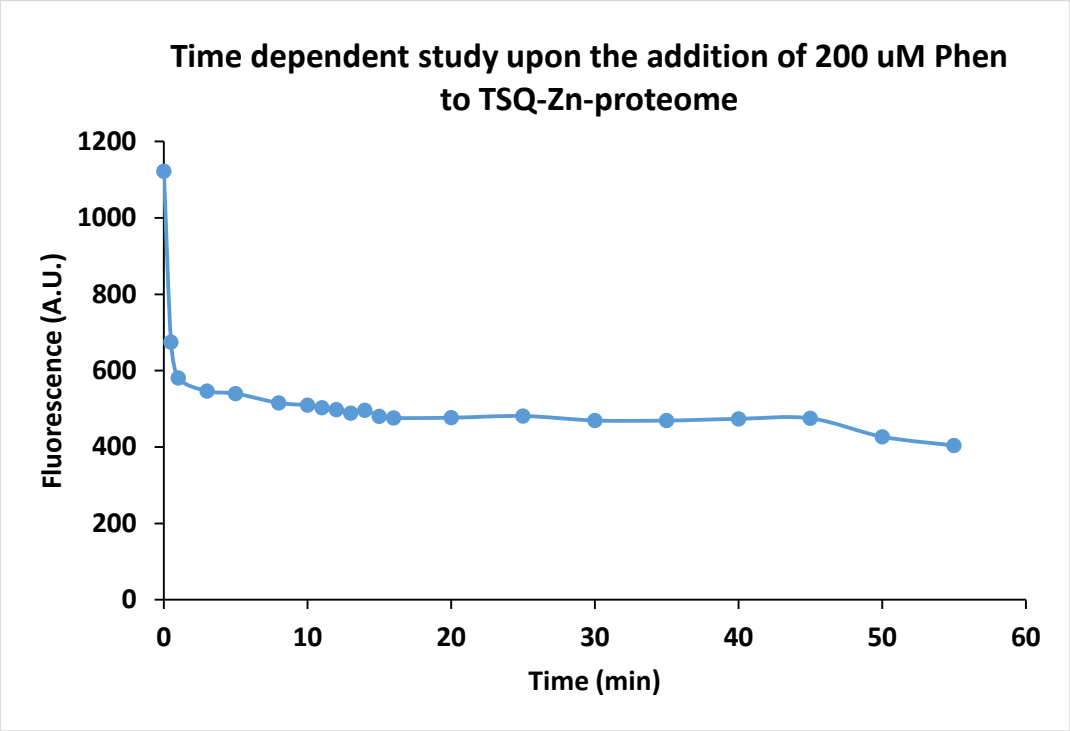

Figure 3.19. Time dependence of reaction of TSQ-Zn-proteome with 1,10-phenanthroline. The nature of the time dependent titration with the adduct of TSQ-Zn-proteome and 200 uM 1,10-phenanthroline in 55 minutes.

Thus, the reaction between 1,10-phenanthroline and Zn-proteome makes adduct formation and maintains an equilibrium. The reaction will proceed in forward direction towards completion if more 1,10-phenanthroline was added.

3.3.3. *Reactions of TSQ with the model protein Alcohol Dehydrogenase*

To further characterize the reaction of TSQ-Zn-proteome with 1,10-phenanthroline, yeast alcohol dehydrogenase was used as a model system. Zn-ADH is a tetramer containing two heterodimers $(Zn_2\alpha\beta)_2$, each dimer has one structural Zn^{2+} and a catalytic Zn^{2+}. First, 8.4 uM of

Zn-ADH in Tris-HCl buffer, pH 7.4 was reacted with 20 uM TSQ and the fluorescence emission spectrum was monitored over the time of 40 minutes. The resulting spectra were centered at 480 nm, that gives a clear indication of the formation of ternary adduct with TSQ, Figure 3.20.

$$\text{TSQ} + \text{Zn-ADH} \rightleftarrows \text{TSQ-Zn-ADH} \qquad (3.9)$$

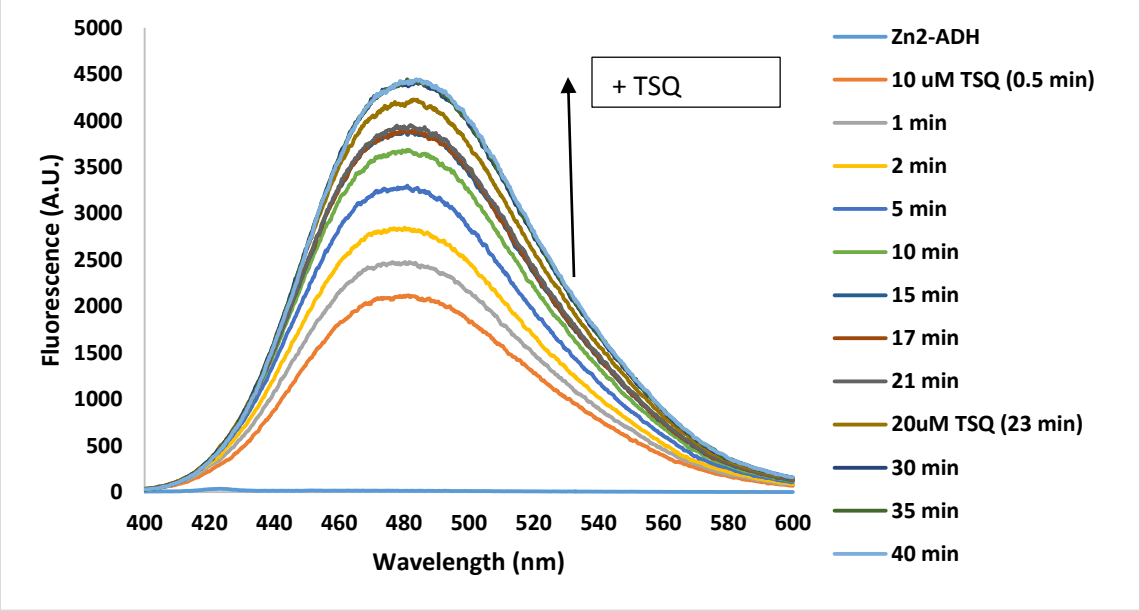

Figure 3.20. Reaction with the model protein Zn-Alcohol Dehydrogenase and TSQ. 8.4 uM Zn-ADH was reacted with 20 uM of TSQ and over the time the fluorescence enhancement was observed until a maximum intensity of fluorescence was obtained in 40 minutes.

Further, the fluorescent product was reacted with the bidentate ligand of interest 1,10-phenanthroline. Upon the addition of 120 uM 1,10-phen, a considerable decrease in the intensity of fluorescence was observed (Figure 3.21). At the same time, the fluorescence was centered at 480 nm. Based on these results, the reaction of 1,10-phen and Zn-ADH could be constructed as follows.

TSQ + Zn-ADH ⇄ TSQ-Zn-ADH (adduct at 480 nm) (3.10)

TSQ-Zn-ADH + 1,10-phenanthroline ⇄ 1,10-phen-Zn-ADH + TSQ (adduct at 480 nm) (3.11)

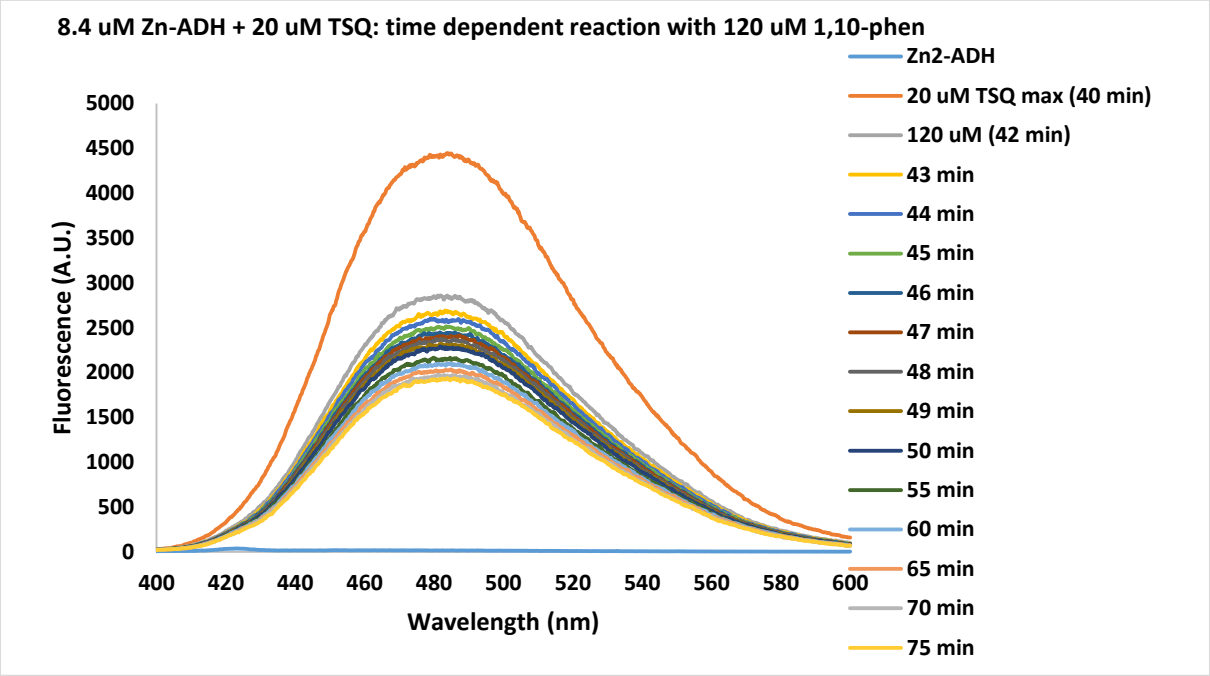

Figure 3.21. Reaction of TSQ treated Zn-ADH with 120 uM 1,10-phenanthroline. 8.4 µM Zn-ADH + 20 µM TSQ in time dependent reaction with 120 µM 1,10-phenanthroline.

The Figure 3.22 below depicts the biphasic kinetics of Zn-ADH treated with TSQ then with the bidentate ligand 1,10-phenanthroline. From the kinetics it is also clear that 1,10-phenanthroline competes with TSQ to displace it and the rate of the initial reaction is very fast. The fact that the reaction does not go to completion suggest that it has come to equilibrium. This is supported by the finding that additional 1,10-phen progressively lowered to final fluorescence intensity.

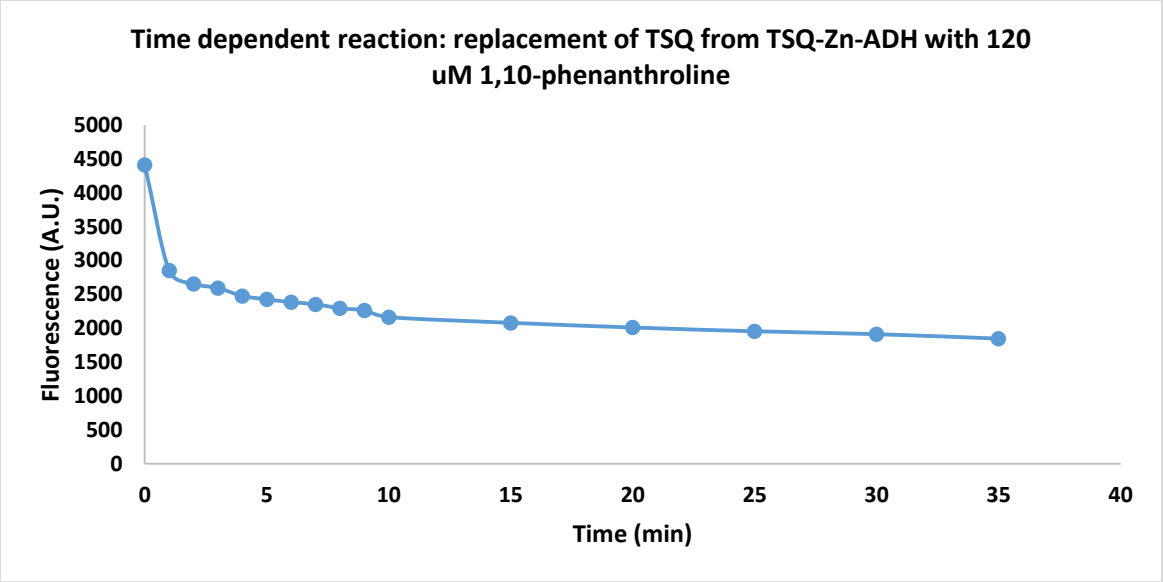

Figure 3.22. Kinetics of the reaction between TSQ-Zn-ADH treated with 1,10-phenanthroline.

After that, the reaction mixture of TSQ, Zn-ADH and 1,10-phenanthroline was chromatographed over the Sephadex G-75 size exclusion column and fifty fractions were eluted. First six fractions collected were called the void fraction volumes. The HMW weight fractions seven to twenty were analyzed for fluorescence. The spectra showed an enhancement in the fluorescence centered at 480 nm. Therefore, ternary complex formation had occurred between TSQ and Zn-ADH. In the presence of 1,10-phenanthroline, the quenching of fluorescence indicated that an adduct of Zn-ADH with 1,10-phen replaced that with TSQ. There was no evidence of fluorescence in the LMW fractions eluted from the Sephadex G-75 column.

In order to determine the Zn^{2+} content in those fractions, Atomic Absorption Spectrophotometry (AAS) was used and the Zn^{2+} content was analyzed for each of the individual

fractions. The combined data of fluorescence and Zn^{2+} content are plotted and displayed below in Figure 3.24. It was demonstrated that the HMW fractions included ternary adducts of 1,10-phen.Zn.ADH and that 1,10-phen did not undergo ligand substitution with Zn-ADH to form $Zn(phen)_2$.

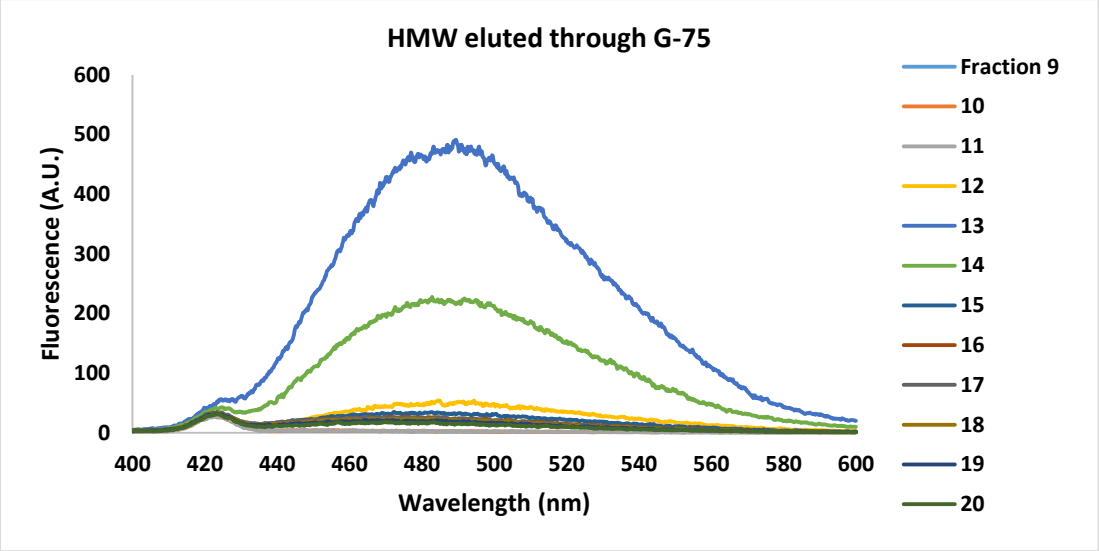

Figure 3.23. Fluorescence emission of Sephadex G-75 fractions of mixture of Zn-ADH+ TSQ +1,10-phenanthroline. The mixture was chromatographed using the Sephadex G-75 column chromatography and HMW fractions were found to display fluorescence centered at 480 nm, suggesting the ternary adduct formation.

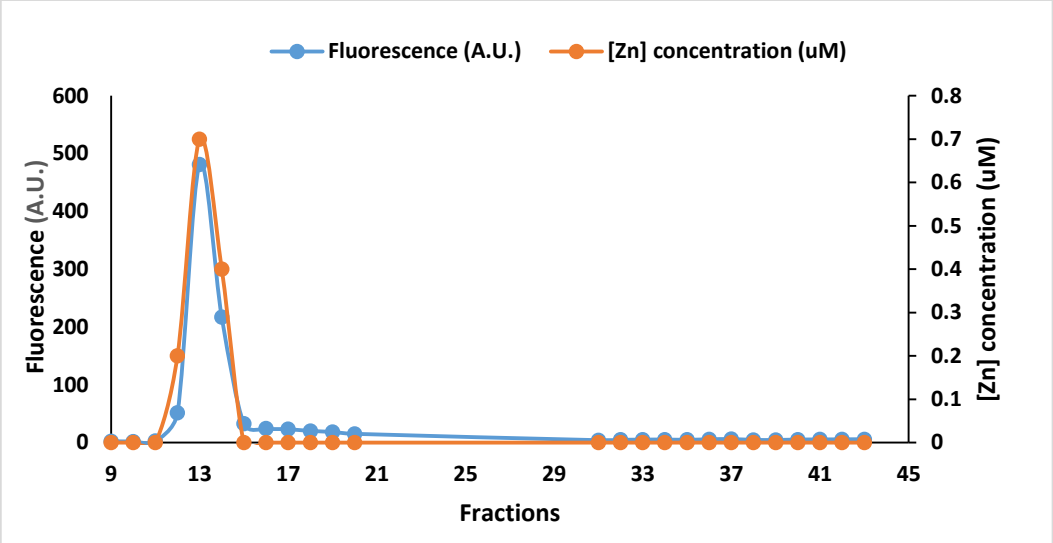

Figure 3.24. Sephadex G-75 of 1,10-phen-Zn-ADH and Zn^{2+} content. The high molecular weight fractions are bound with zinc.

From both the experimental results, using the Zn-proteome and using the model protein Zn-ADH, it is confirmed that the ligand of interest 1,10-phenanthroline competes with TSQ, displaces the fluorophore from its Zn-binding sites, and forms the ternary adduct of 1,10-phen-Zn-ADH.

3.4. *Reaction of phen-Zn-proteome with TSQ*

3.4.1. E*xperiments with Zn-proteome*

1,10-phenanthroline can compete to displace the fluorophore TSQ from the ternary adduct of TSQ-Zn-proteome resulting in an equilibrium mixture. The present experiment was designed to investigate the opposite reaction. In order to examine this reaction, Zn-proteome was collected and the Zn^{2+} concentration was measured using AAS. One milliliter of 9.2 uM of Zn-proteome (in terms of Zn^{2+} concentration) was reacted first with 18 uM of TSQ and monitored

for fluorescence enhancement. Upon reaching a stable, maximum fluorescence intensity within 1 hour, the data were recorded and displayed below in Figure 3.25. The fluorescence emission maximum was centered at 470 nm, that indicated the formation of TSQ-Zn-proteome.

$$\text{Zn-proteome} + \text{TSQ} \rightleftarrows \text{TSQ-Zn-Proteome} \qquad (3.12)$$

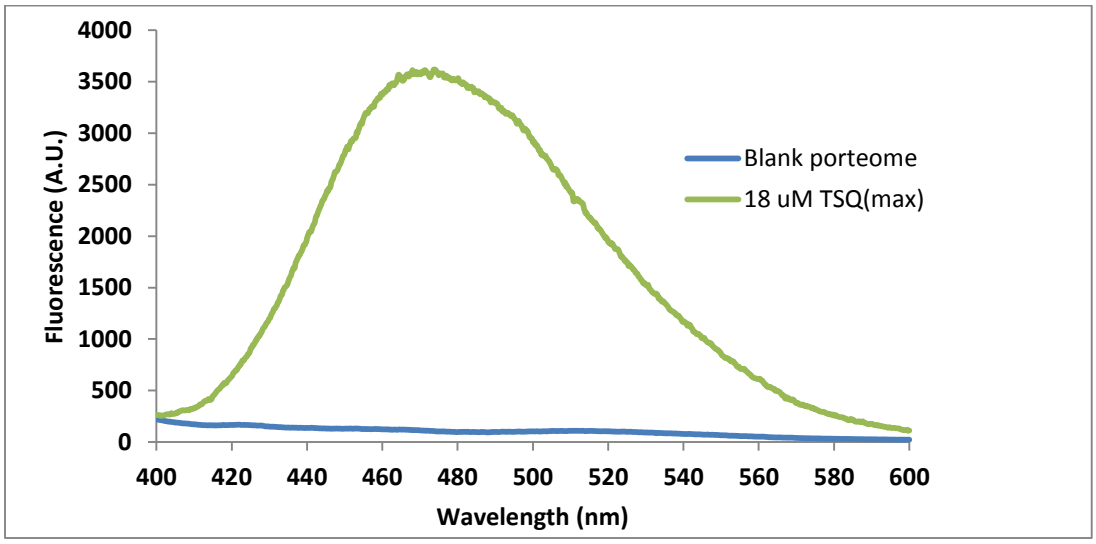

Figure 3.25. The fluorescence of 9.2 uM Zn-proteome treated with 18 uM TSQ. One mL 9.2 uM Zn-proteome was allowed to react with 18 uM TSQ. The fluorescence change was recorded.

At the same time a parallel experiment was carried out using another aliquot of 9.2 uM Zn-proteome that was treated with 100 uM of 1,10-phenanthroline keeping the total volume one mL. The solution was mixed well using a plastic pipetter and kept in dark on ice for two hours. Subsequently, the reaction mixture analyzed by spectrofluorimetry. 1,10-phenanthroline is not a fluorophore, so only background fluorescence was observed. Then the mixture was treated with 18 uM TSQ to determine whether 1,10-phenanthroline makes any ternary adduct formation with

Zn-proteome that competes with TSQ. Over time a fluorescence emission spectrum was a wavelength maximum centered at 470 nm developed indicating formation of TSQ-Zn-proteome due to the displacement of 1,10-phenanthroline (Figure 3.26). The lower intensity of fluorescence in comparison with the control of Zn-proteome plus TSQ was due to the equilibrium formation of the mixture of TSQ-Zn-proteome and 1,10-phen-Zn-proteome. TSQ still needs longer time to completely displace all the 1,10-phen from the ternary adduct of 1,10-phen-Zn-proteome.

The spectrum could be interpreted in terms of the following reactions:

Zn-proteome+1,10-phen ⇄ 1,10-phen-Zn-proteome (3.13)

(non-fluorescent adduct)

1,10-phen-Zn-proteome+TSQ⇄TSQ-Zn-proteome+1,10-phen (3.14)

(ternary adduct at 470 nm)

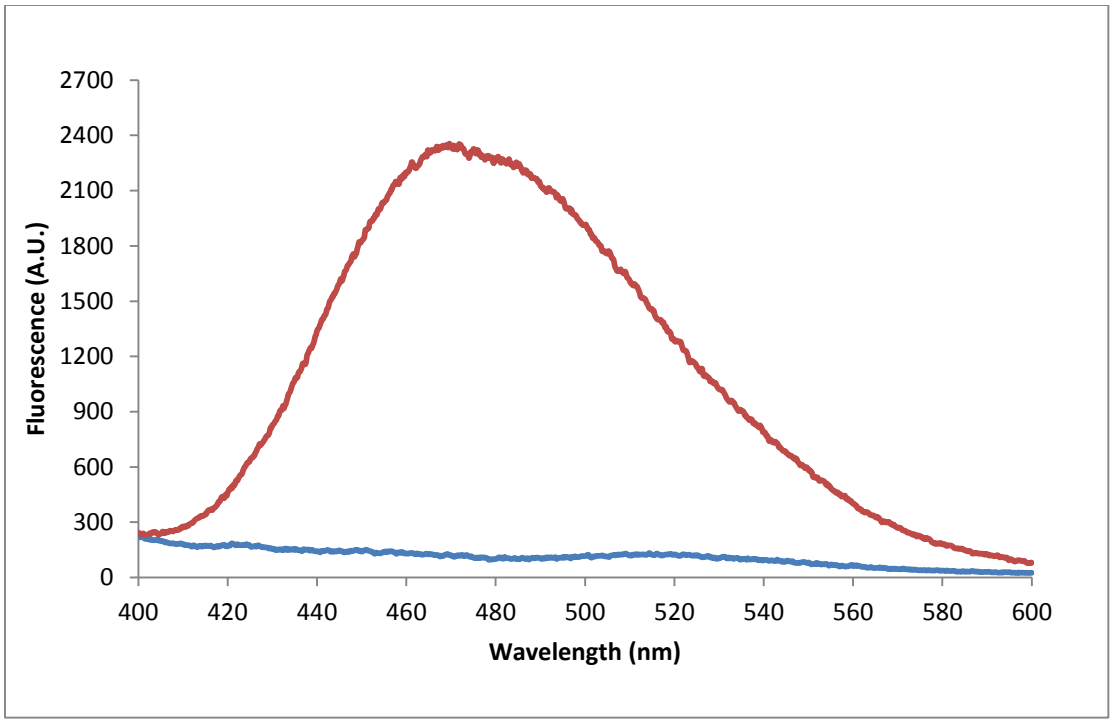

Figure 3.26. 1,10-phenanthroline treated with Zn-proteome and subsequent reaction upon TSQ addition. 9.2 uM Zn-proteome was incubated with 100 µM 1,10-phen then reacted with 18 uM TSQ (in 70 minutes max).

3.4.2. *A parallel set of experiments with Alcohol Dehydrogenase*

Another set of experiments was carried out to test whether the final state of the reaction of Zn-ADH with TSQ and 1,10-phenanthroline was independent of the order of addition. A freshly prepared solution of Zn-ADH in Tris-Cl buffer, pH 7.4 at 25°C was assessed for Zn^{2+} content by AAS. A concentration of 11 uM Zn^{2+} in the Zn-ADH was measured. Treating the protein with 20 uM TSQ for an hour yields the maximum fluorescence (Figure 3.27). Immediately the mixture was treated with 100 uM of 1,10-phenanthroline. A sharp and immediate decrease in fluorescence was observed and monitored until about an hour to reach equilibrium (Figure 3.27). Approximately 40% decrease in the fluorescence decay was detected.

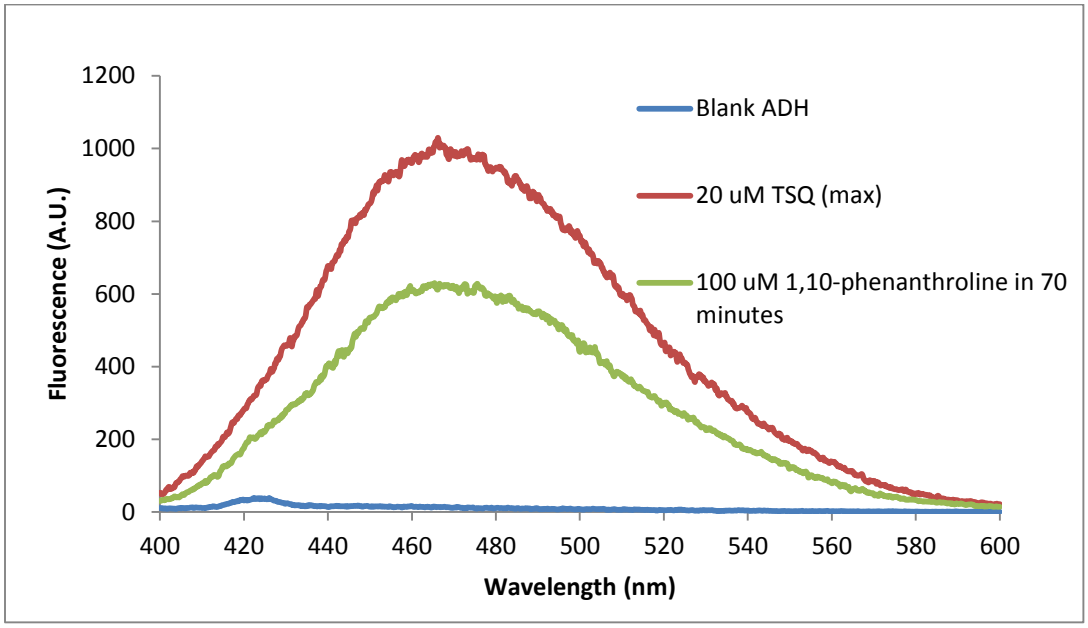

Figure 3.27. The reaction of Zn-ADH + TSQ + 1,10-phenanthroline. 11 uM Zn-ADH (in terms of Zn^{2+} concentration) was reacted with 20 uM TSQ, subsequently the reaction mixture was treated with 100 uM 1,10-phenanthroline. A ternary adduct formation of 1,10-phen-Zn-ADH was observed based on the displacement of TSQ and fluorescence emission maximum centered at 470 nm.

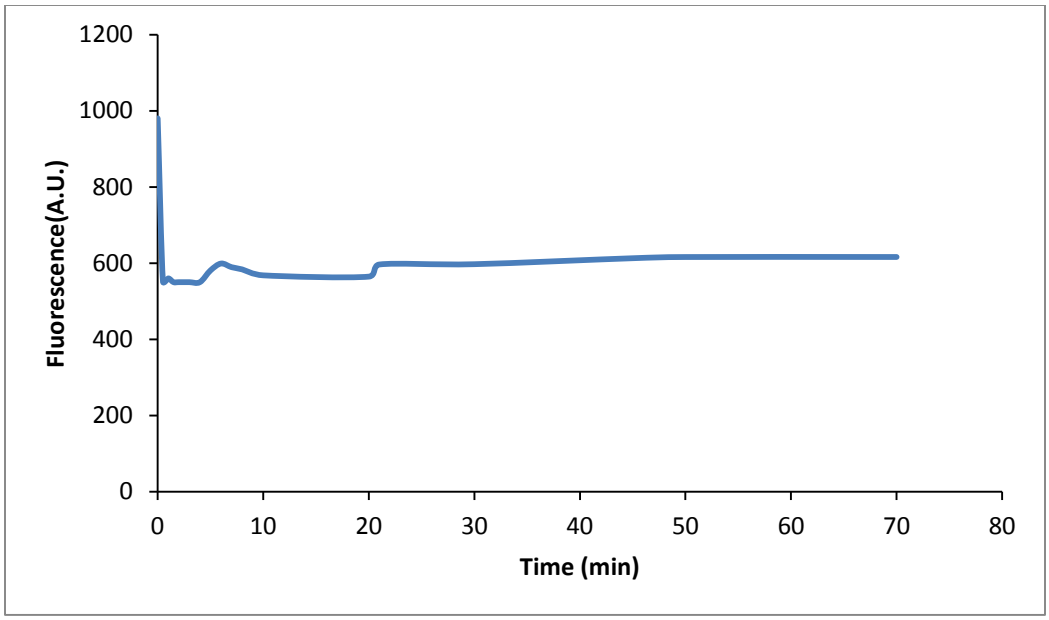

Figure 3.28. Diagram of Fluorescence vs. time (minute) plot. 11 uM Zn-ADH was reacted with 20 uM TSQ. After the completion of this reaction 100 uM Phen was added and fluorescence change was recorded.

At the same time, in a separate cuvette, the same stock solution 11 uM Zn^{2+} containing in Zn-ADH was treated with 100 uM of 1,10-phenanthroline and incubated in dark for two and half hours. Afterwards, because 1,10-phen-Zn-ADH is a non-fluorescent adduct, only a baseline was recorded. Upon the addition of 20 uM TSQ, the maximum fluorescence intensity enhancement was recorded, Figure 3.29. The final fluorescence intensity matched that in Figure 3.27.

The results of this experiment are consistent with rapid kinetics in either direction of the following reaction. The reactions of this experiment can be described as follows.

i) Zn-ADH + TSQ ⇄ TSQ-Zn-ADH (3.15)
(fluorescence at 470 nm)

TSQ-Zn-ADH+ 1,10- Phen ⇄ Phen-Zn-ADH+ TSQ (3.16)

(reduced fluorescence)

ii) Zn-ADH + 1,10- Phen ⇄ Phen-Zn-ADH (3.17)
(non-fluorescent adduct)

Phen-Zn-ADH + TSQ ⇄ TSQ-Zn-ADH (3.18)
(enhanced fluorescence at 470 nm)

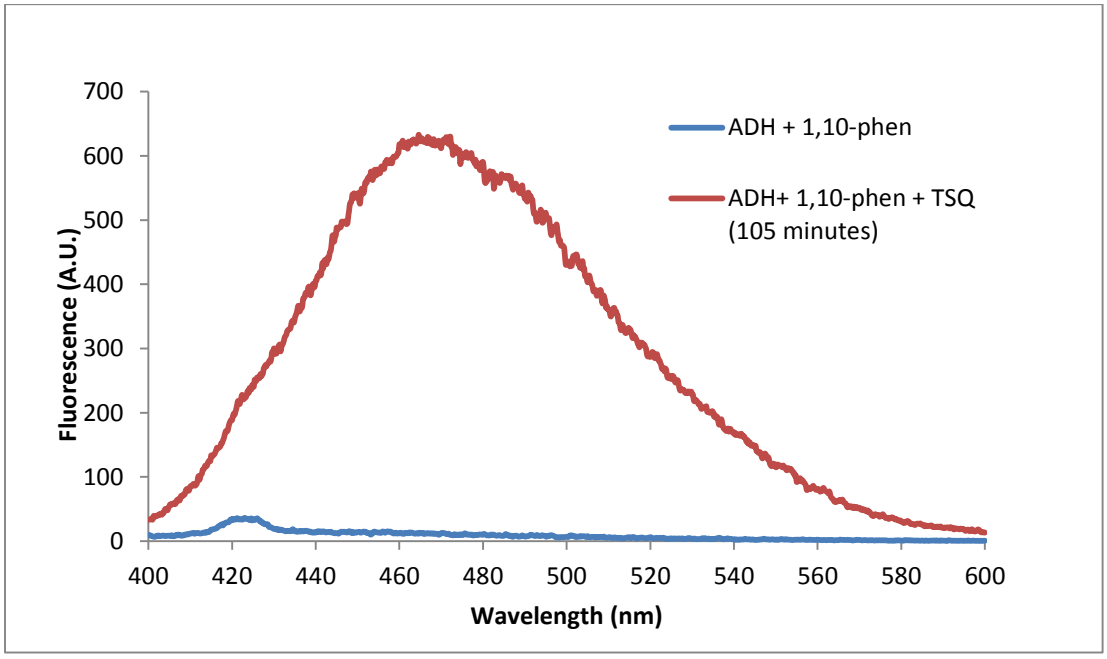

Figure 3.29. The reverse addition of 1,10-phen with Zn-ADH then the reaction with TSQ. 11 uM Zn-ADH (in terms of Zn^{2+} concentration) was reacted with 100 uM 1,10-phenanthroline. After 2.5 hours 20 uM TSQ was added and the maximum fluorescence intensity was recorded.

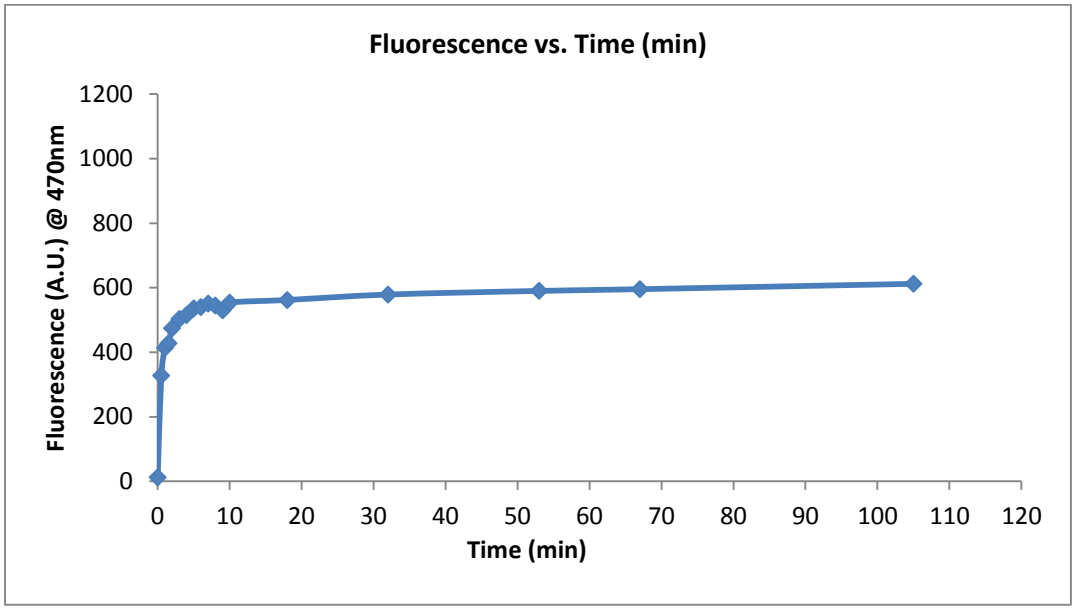

Figure 3.30. The kinetics of reaction 3.15 & 3.16 described in Figure 3.28. After the TSQ was added, the fluorescence intensity was monitored for nearly 2 hours to see the maximum stable fluorescence.

3.5. *Enzyme Activity Assay*

To understand more clearly whether the bidentate ligand 1,10-phenanthroline react with the model protein Zn-ADH, an enzyme activity assay was performed. The assay was performed by using in 20 mM Tris-Cl buffer, pH 7.4 at 25°C containing 1.5 mM NAD, 0-450 mM EtOH and 19.5 uM of Zn-ADH. The conversion of NAD to NADH was signified by an increase in absorbance at 340 nm. The initial rate was monitored at 340 nm for 15 seconds. Treatment of the ligand with 1,10-phenanthroline at a concentration of 50 uM and 80 uM showed reduced activity of the enzyme by 25% and 50% respectively, still retaining 75% and 50% of its catalytic activity in terms of the increased concentration with the addition of 1,10-phen. These experimental data additionally allow in support to conclude that the ligand 1,10-phenanthroline

is able to react with the enzyme Zn-ADH, and plays a significant role in the inhibition of the enzyme by showing decreased absorbance when treated with the ligand and follows a Michealis-Menten kinetics (Figure 3.31).

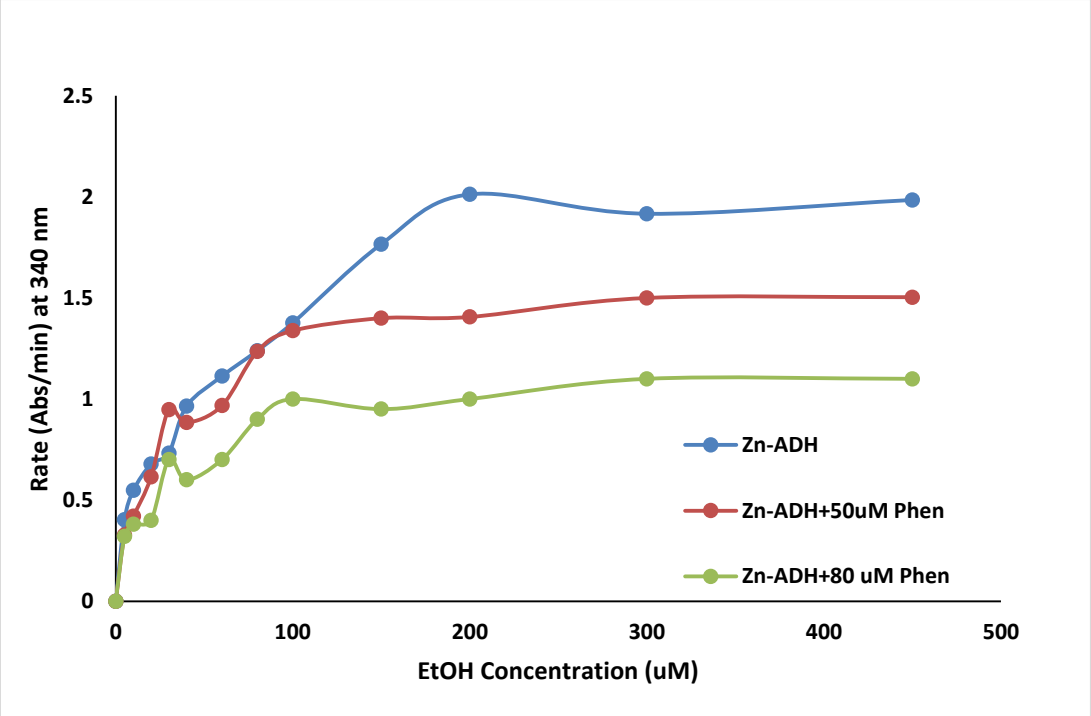

Figure 3.31. Enzyme activity assay of Zn-ADH. The assay was performed in 20 mM Tris-Cl pH 7.4 at 25°C containing 1.5 mM NAD, 0-450 mM ethanol and 19.5 uM of the enzyme Zn-ADH (in terms of Zn^{2+} concentration). Initial rate was monitored at 340 nm for 15 seconds. Results were compared with the enzyme ADH and not-reacted 1,10-phenanthroline.

3.6. *TSQ Staining of NSDS-PAGE gels and the reaction of Zn-proteome with TSQ and 1,10-phenanthroline*

The proteomic Zn^{2+} competition for adduct formation between TSQ and 1,10-phen has been demonstrated. Next, competition at the individual Zn-proteome level was investigated. Sodium dodecyl sulfate polyacrylamide gel electrophoresis (SDS-PAGE) is the most commonly used technique to obtain high resolution separation of analytical mixtures of proteins.[43] But the SDS-PAGE method does not keep the proteome in its native state along with its metal cofactors. For the purpose of maintaining the integrity of the proteome, we used Dr. Andrew Nowakowski's technique of Native SDS-PAGE high resolution electrophoretic separation (NSDS-PAGE) of proteins with retention of native properties including bound metal ions.[43] To begin the study, 5 X 10^8 LLC-PK_1 cells grown in culture and collected, lysed via sonication, and 500 mM phenylmethylsulfonyl fluoride (PMSF) and 1000 U Benzonase © nuclease (Sigma) were added to inhibit proteolysis and increase nuclease activity, respectively. The sonicate was centrifuged at 47 000 X g for 30 minutes at 4^{o}C. The supernatant was run over a Sepahadex G-25 gel filtration column using degassed 5mM Tris-Cl buffer, pH 8.0. The HMW proteome fractions exhibiting absorbance at 280 nm were pooled together and subsequently loaded onto a Macro-Prep DEAE-HPLC anion exchange column (Bio-Rad) for further separation. The column was eluted with 5 mM Tris-Cl pH 8.0 with a step gradient from 0-500 mM NaCl. The fractions eluted from the DEAE-HPLC column separation were measured for conductance and absorbance at 280 nm (See Figure 3.32). Select fractions were concentrated using a Millipore centrifuge filter (3000 Da molecular weight cut-off) that was spun at 12,000 X g for 20 minutes at 4^{o}C. Samples were desalted by

repeating the concentration three times, washing the protein samples with fresh 5 mM Tris-Cl pH 8.0 between each concentration.

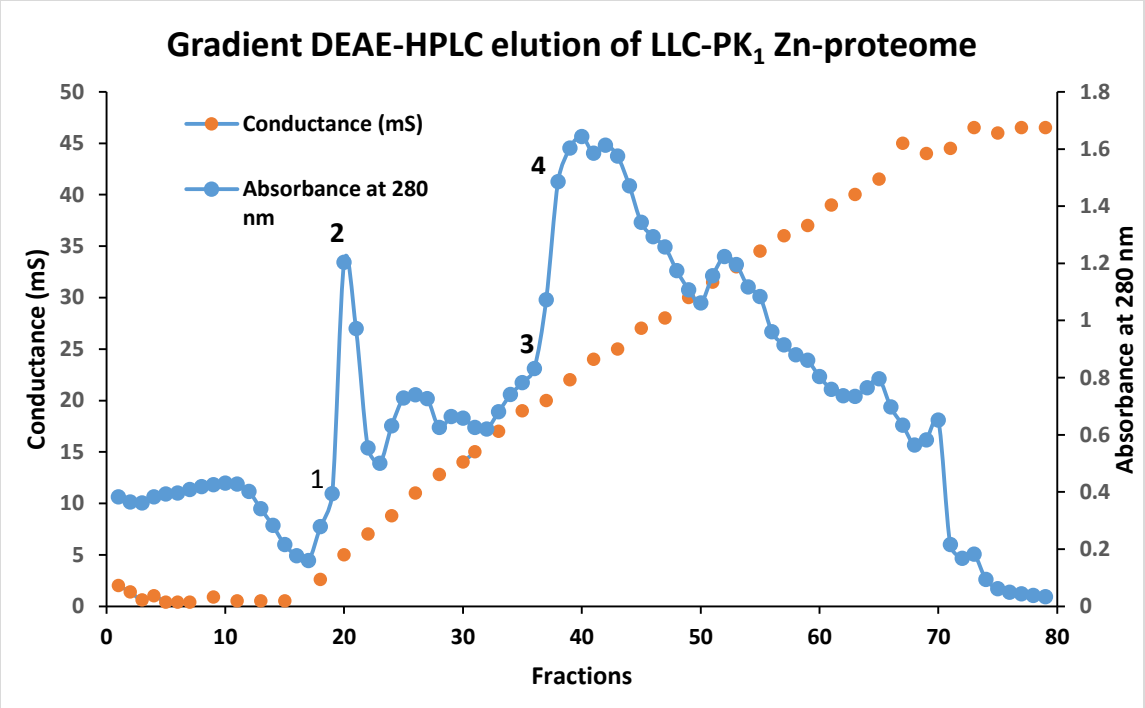

Figure 3.32. Gradient DEAE elution of isolated LLC-PK$_1$ proteome: Isolated LLC-PK1 proteome in 5 mM Tris-Cl pH 8.0 was loaded onto a 5 mL Macro-Prep DEAE column. The column was eluted step wise 0-500 mM NaCl up to final concentration 500 mM NaCl in 5 mM Tris-Cl pH 8.0. Conductivity and absorbance at 280 nm were recorded.

In order to understand and clearly see the effect of 1,10-phenanthroline and its adduct formation properties with the isolated Zn-proteins, selected fractions from the gradient elution were loaded onto in a NuPAGE Novex 12% Bis-Tris 1.0 mm minigels (Invitrogen) and electrophoresed using the NSDS-PAGE method. After the electrophoresis was complete, the cassette was separated and the gel was taken out and washed with 100 mL ddH_2O.

For TSQ staining, gels were soaked in 50 mL of ddH_2O containing 25 mM TSQ on a rotary shaker for 40 minutes and washed twice with fresh ddH_2O for 5 minutes before fluorescent images were recorded (See Figure 3.33(A)). Gels were then additionally incubated in 50 mL of ddH_2O containing 200 µM 1,10-phenanthroline for 30 minutes before subsequent images were captured (See Figure 3.33(B).

To visualize the results of the reaction of separated Zn-proteome with TSQ and then 1,10-phen, the reacted gel were transferred to a UVP EpiChemi II Darkroom UV transilluminator gel box and excited at 365 nm (long wavelength UV setting), the excitation wavelength of TSQ. Fluorescent images were recorded with a digital camera with a 470 nm emission filter using a three second exposure time.

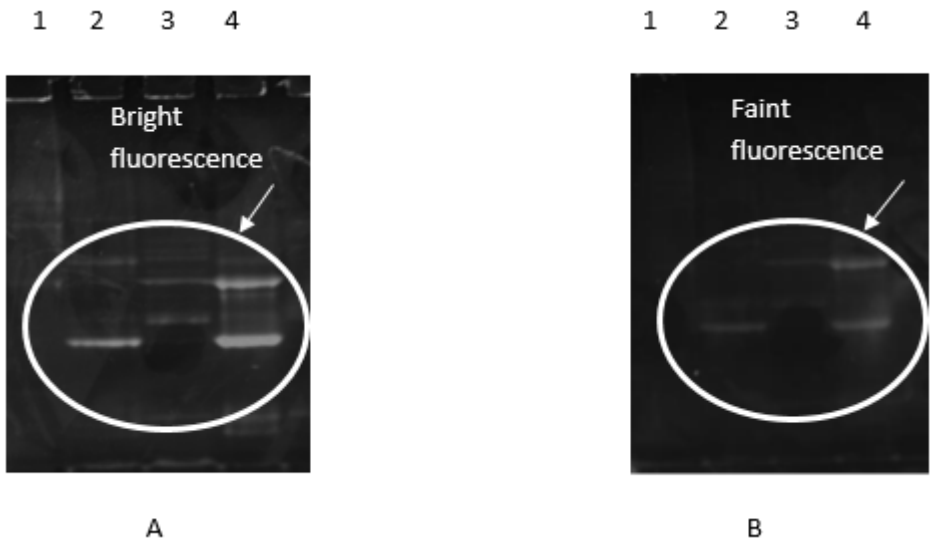

Figure 3.33. Imaging of the reaction of 1,10-Phen with TSQ-Zn-Proteins. DEAE fractions of proteome were separated by the method of Native SDS-PAGE that retains protein bound Zn^{2+}. In A selected bands of Zn-proteome fluoresce brightly when stained with 25 µM TSQ. In B, after the reaction with 200 µM 1,10-phentharoline the brightly fluoresced bands with TSQ is quite faint, that supports of the adduct formation of Phen-Zn-proteome replacing TSQ from the adduct of TSQ-Zn-proteome.

According to Figure 3.33(A) it is evident that some of the bands show bright fluorescence with TSQ. However, these bands were mostly quenched after the reaction with 200 µM 1,10-phenanthroline. This experiment specifically supports the conclusion that both TSQ and 1,10-phenanthroline are able to make adducts with specific proteins in the Zn-proteome.

3.7. *Cellular Quenching of TSQ Fluorescence using Glutathione (GSH)*

Cellular glutathione is an important tripeptide Figure 3.34. GSH plays an important role as an antioxidant in plants, animals, fungi and some other bacteria and archea, preventing damage to important cellular components caused by reactive oxygen species such as free radicals and peroxides.[45] It does so through its sulfhydryl group in its chemical structure; thiol (-SH) groups are reducing agents. GSH exists in the concentration range of 1-10 mM in animal cells.[46]

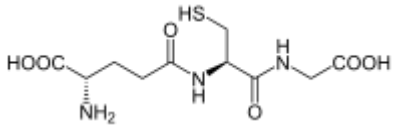

Figure 3.34. Chemical structure of glutathione

In the current experiments, glutathione was used as a ligand to see if it has any binding capacity with the cellular Zn-proteins. To begin, in accordance with the previous chapter-1 of this thesis, we used the TSQ-Zn-proteome as a reporter to study the binding of ligands to the Zn-proteome. The same hypothesis was applied here. If Glutathione reacts in the cellular level with Zn-proteome, the effect can be monitored upon ligand substitution for the sensor TSQ from the ternary adduct of TSQ-Zn-proteome. The reaction could be described as follows:

$$\text{Zn-proteome} + \text{TSQ} \leftrightarrows \text{TSQ-Zn-proteome (470 nm)} \quad (3.19)$$

$$\text{TSQ-Zn-proteome} + \text{GSH (reduced)} \leftrightarrows \text{GS-Zn-proteome} + \text{TSQ (470 nm)} + H^{+} \quad (3.20)$$

When one mL of 4.5 uM Zn-proteome was reacted with 10 uM of TSQ a maximum fluorescence emission was attained in about 70 minutes due to the formation of TSQ-Zn-proteome. Figure 3.35 shows the fluorescence spectrum of the ternary adduct centered at 472 nm. The ternary adduct of TSQ-Zn-proteome was subsequently used to monitor the effect of the reaction of glutathione (GSH) with Zn-proteome.

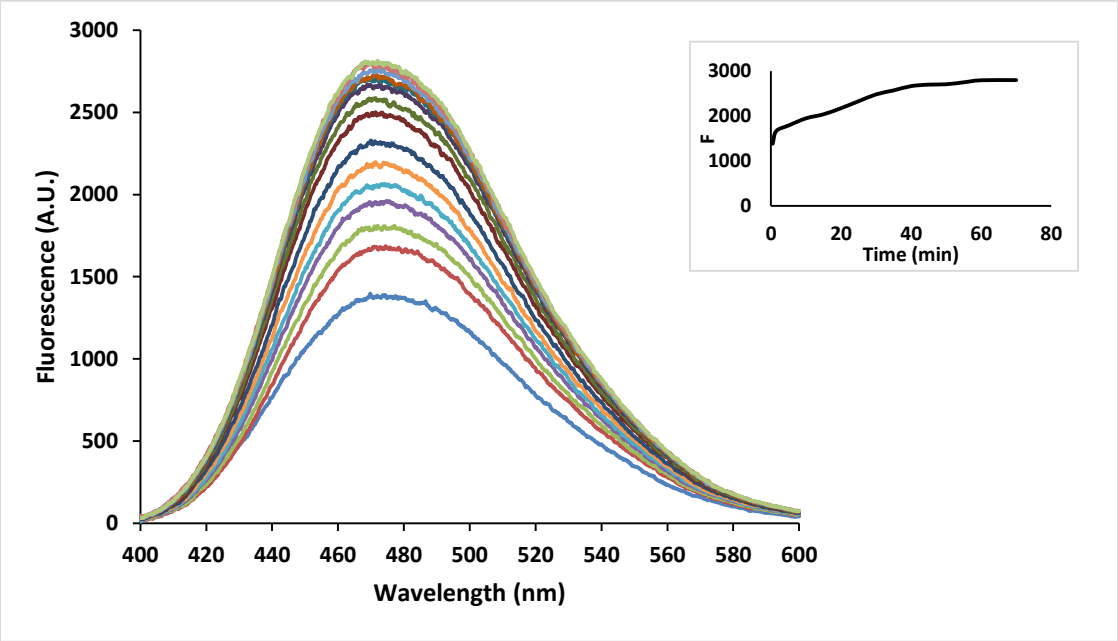

Figure 3.35. Time dependent reaction of Zn-proteome with TSQ. One mL of Zn-proteome (4.5 uM Zn^{2+}) was titrated with 10 uM of TSQ over the time of 70 minutes. A stock concentration of 2 mM TSQ (in DMSO) was used for the experiment.

A stock solution of 10 mM glutathione (GSH) was prepared in 15 mL 20 mM degassed Tris-Cl, pH 7.4 keeping the solution at room temperature. Titration of TSQ-Zn-proteome with glutathione started at 50 uM and increased gradually to 1.15 mM. Figure 3.36 displays the whole reaction, which was carried out over 2.5 hours. The fluorescence quenching happens in a biphasic manner

without changing in the remaining fluorescence spectrum. From the data of Figure 3.37, it is evident that glutathione competes to replace TSQ resulting in the gradual loss of the intensity of TSQ-Zn-proteome resulting in the formation of GS-Zn-proteome.

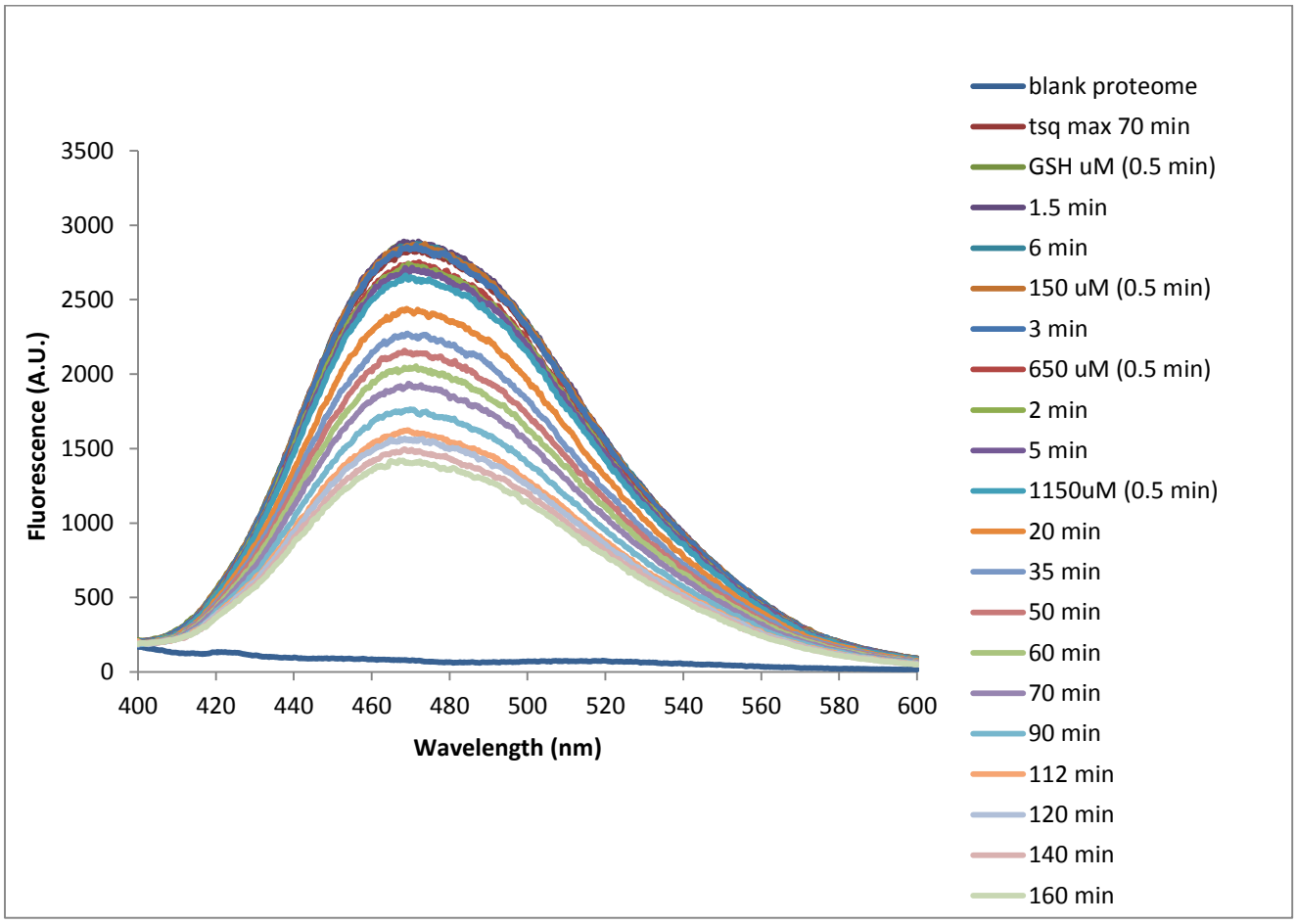

Figure 3.36. The ternary adduct TSQ-Zn-proteome was titrated with Glutathione (GSH). A 10 mM Glutathione (GSH) solution was prepared in 20 mM Tris-Cl, pH 7.4. A total of 1.15 mM concentration of glutathione was added and time dependent changes in fluorescence were recorded.

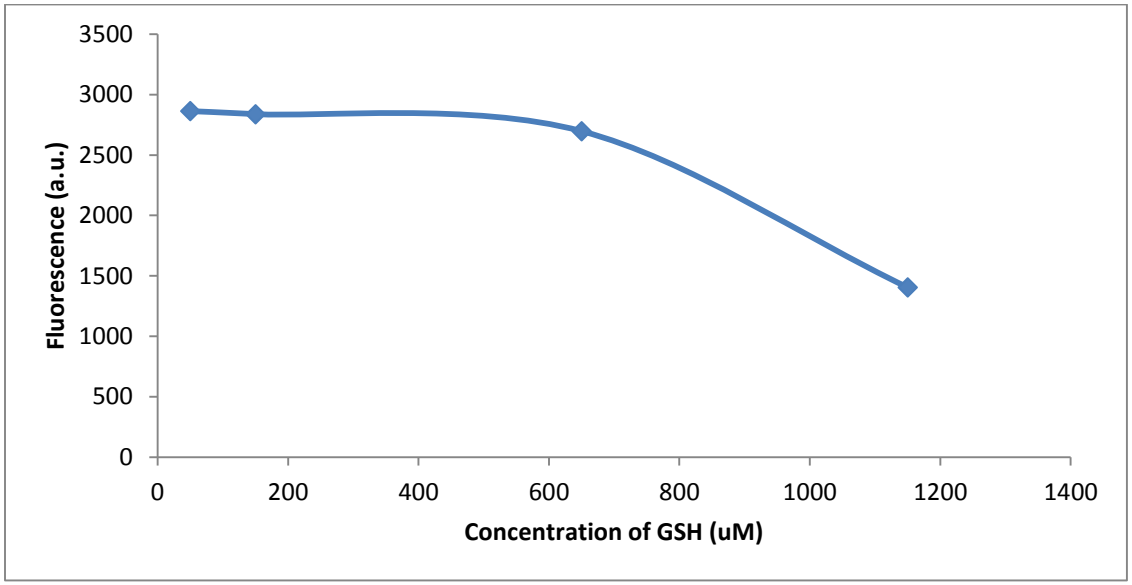

Figure 3.37. Concentration dependence of the reaction of TSQ-Zn-proteome with GSH.

3.8. *Cellular Chemistry of TCEP (tris(2-carboxyethyl)phosphine)*

After finding evidence from the reaction of glutathione with TSQ-Zn-proteins that GSH forms a ternary adduct with Zn-proteins, other plausible ligands such as Histidine, 8-Hydroxyquinoline, Dimethyldithiocarbamic acid and TCEP (Tris(2-carboxyethyl)phosphine) were studied. The first was TCEP, which is used as a reducing agent to keep protein thiols from oxidizing to disulfides.

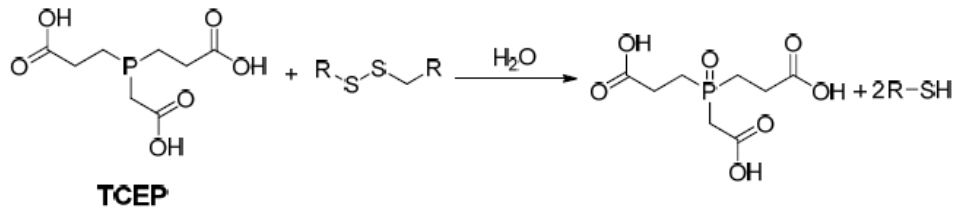

TCEP

(3.21)

Glutathione reduces disulfide bonds formed within cytoplasmic proteins to cysteines in that disulfide exchange, redox reaction. In the process, glutathione is converted to its oxidized form glutathione disulfide (GSSG). The reaction could be expressed as follows.

$$2\ GSH + R\text{-}S\text{-}S\text{-}R \leftrightarrows GS\text{-}SG + 2RSH \qquad (3.22)$$

There has been much research to find a chemical that could serve as an effective thiol protectant compound. TCEP has recently been introduced and is commercially available as such a reagent.[47] The properties of TCEP have been attractive especially in studies of proteins which can be sensitive to sulfhydryl oxidation. TCEP carries three carboxyl groups in its structure and these carboxyl groups might serve as a multidentate ligand that bind to Zn-proteins.

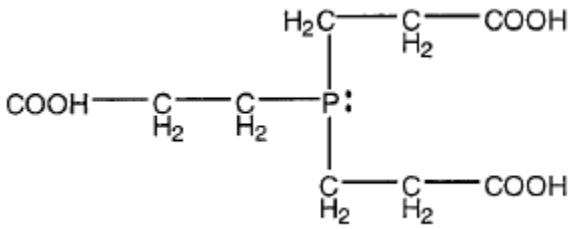

Figure 3.38: Chemical structure of TCEP

Experiments were undertaken to investigate whether TCEP does also exhibit binding properties with the Zn-proteome. To investigate this novel hypothesis, the following experiments were carried out.

TCEP is stable in aqueous solution at pH values above 7.5.[48] TCEP was dissolved in 20 mM Tris-Cl buffer, pH 7.4 and a 68 mM stock solution was prepared. At first, a control experiment was run to determine if TCEP makes a complex formation with the Zn^{2+} solution. For this reaction, 10 uM

of TSQ was reacted with 10 uM Zn^{2+} making a total volume of one mL in a cuvette to study fluorescence, with excitation wavelength at 370 nm. The reaction was monitored over the time for 40 minutes, and a maximum fluorescence was observed and recorded. According to Figure 3.39, the spectrum was recorded with the maximum intensity of fluorescence centered at 490 nm, consistent with the formation of $Zn(TSQ)_2$. Subsequently, the product was titrated with TCEP, taking aliquots from the stock solution of 68 mM. From the Figure 3.39 it is indicative that 0 - 1.18 mM TCEP modestly quenched the intensity of the fluorescence without changing fluorescence maxima that was centered at 490 nm. This result suggested that TCEP formed a complex with Zn^{2+} that was less stable than $Zn(TSQ)_2$.

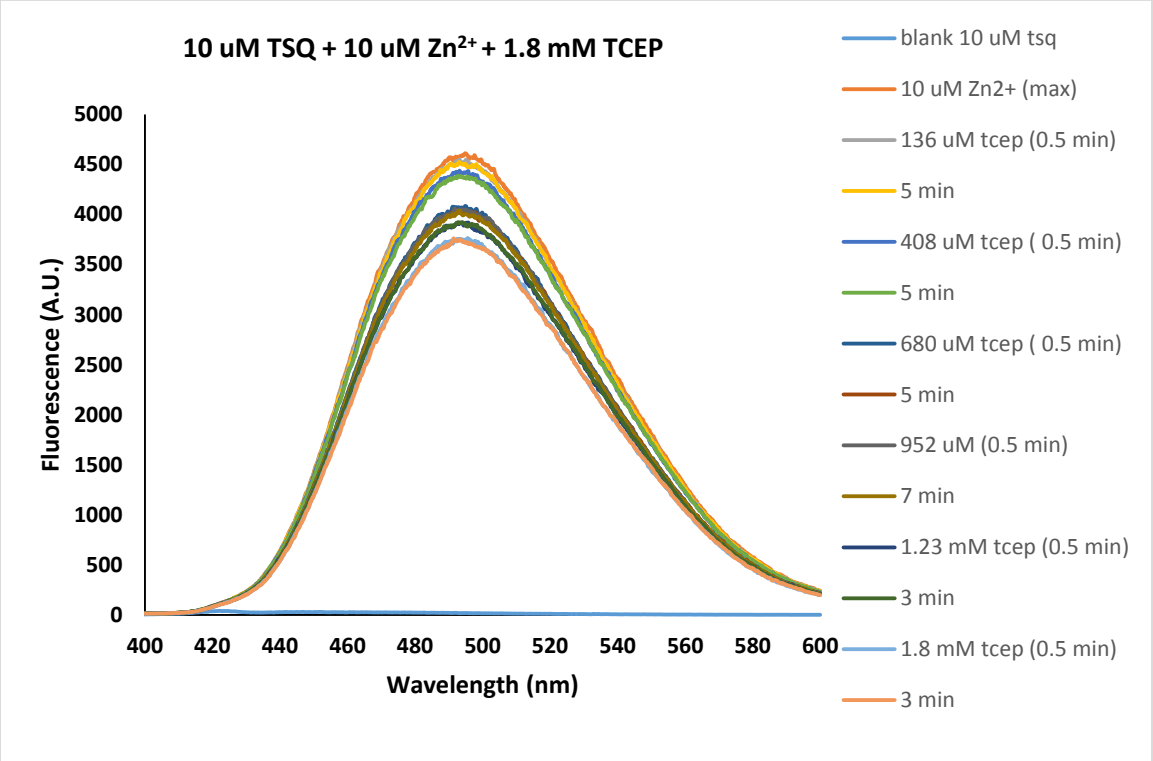

Figure 3.39. Titration of $Zn(TSQ)_2$ complex with TCEP. A total of 1.18 mM concentration of TCEP was added over 30 minutes.

3.8.1. *The cellular chemistry of TCEP with LLC-PK$_1$ cell lysate*

LLC-PK$_1$ cell lysate not only consists of the Zn-proteome but it also contains small molecular size peptides such as glutathione. The previous experiment with GSH indicated that it can form adducts with components of the Zn-proteome. Thus, in the cell lysate some of the glutathione may be reversibly stay bound as ternary adducts with Zn-proteins. In that case, of cell lysate, if the fluorophore TSQ added to lysate to image out Zn-proteins, Glutathione (GSH) may partially inhibit the availability of the Zn-proteome to react with TSQ. On the other hand, if TCEP is injected in the cell lysate, it will prevent glutathione from being oxidized and will help retain the Zn-proteome in its native reduced state react upon the addition of TSQ.

If this hypothesis is correct, a reduced amount of fluorescence intensity might be resulting in for the reaction of TSQ with Zn-proteome when the cell lysate is treated with TCEP. The idea could be presented as the following reactions in light of the presence of TCEP.

Cellular GSH + Zn-proteome ⇆ GS-Zn-proteome (3.23)

Zn-proteome + TSQ ⇆ TSQ-Zn-proteome (fluorescent emission at 470 nm) (3.24)

Based on the hypothesis, an experiment was carried out growing 10 plates (10X10^8 cells) of LLC-PK$_1$ cell lines in the Media M199. After the cells reached confluence, they were harvested using DPBS, then sonicated and centrifuged using Sorvall SS-34 for 20 minutes. The cell supernatant was collected and diluted to total volume of 3 mL using 20 mM Tris-Cl buffer, pH 7.4. From the diluted supernatant cell lysate, two parallel experiments were run.

i) One mL of the LLC-PK_1 cell lysate containing 10 uM Zn^{2+} concentration was treated with 1 mM TCEP (from 68 mM stock solution) and kept in the dark for an hour. Then it was exposed to 10 µM TSQ.

ii) Another one mL aliquots of the LLC-PK_1 cell lysate, containing the same 10 uM Zn^{2+} concentration was used directly for the reaction with the fluorophore TSQ.

Part-i: *LLC-PK_1 cell lysate treated with TCEP*

The LLC-PK_1 cell lysate treated with 1 mM TCEP was titrated with TSQ in two separate additions of 10 uM and a total of 20 uM concentration of TSQ was added using from a stock solution of 5 mM TSQ. In the following Figure 3.40 the results were plotted. The fluorescence intensity was later compared with the cell lysate without treated with TCEP (see part ii).

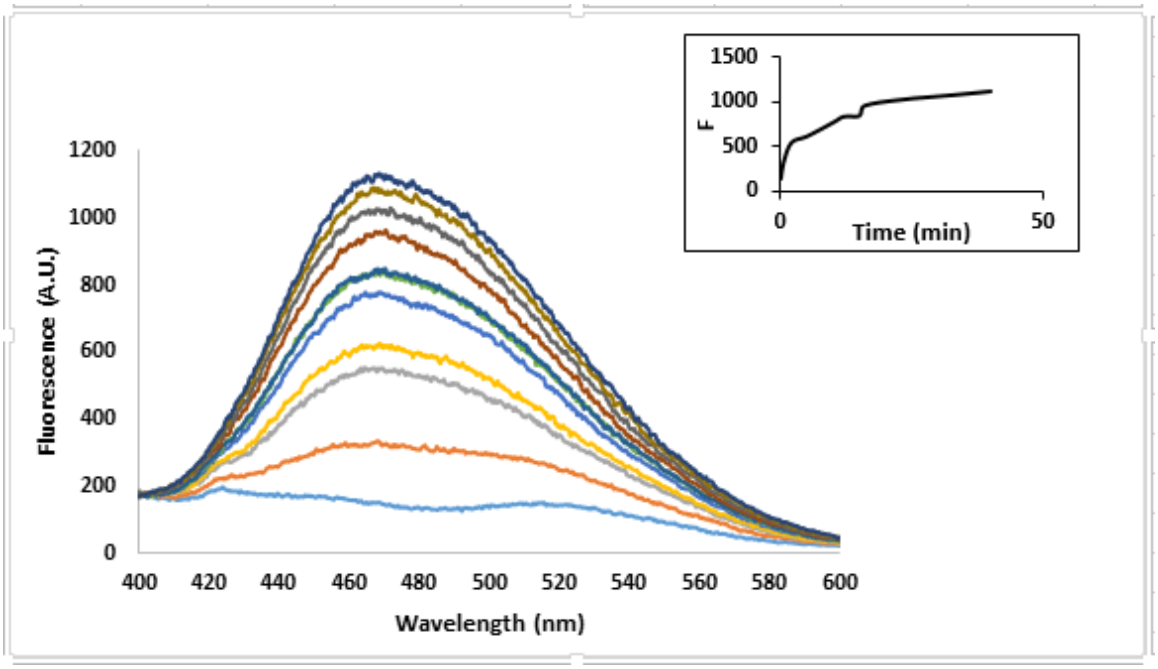

Figure 3.40. Reaction of TCEP (1 mM) treated LLC-PK$_1$ cells exposed to TSQ. One mL LLC-PK$_1$ cell lysate was treated with 1 mM TCEP then stepwise reacted with up to 20 uM TSQ and the changes in the fluorescence intensities were recorded.

The ternary adduct formation, results in TSQ-Zn-proteome, was eluted through Sephadex G-75 gel filtration column and 40 fractions were collected. After eluting the reaction mixture, all the fluorescence (Figure 3.41) and Zn^{2+} concentration (Figure 3.42) was found located in the high molecular weight (HMW) proteomic region. The fluorescence wavelength maximum remained at 470 nm, Figure 3.41, which further supporting the formation of a ternary adduct.

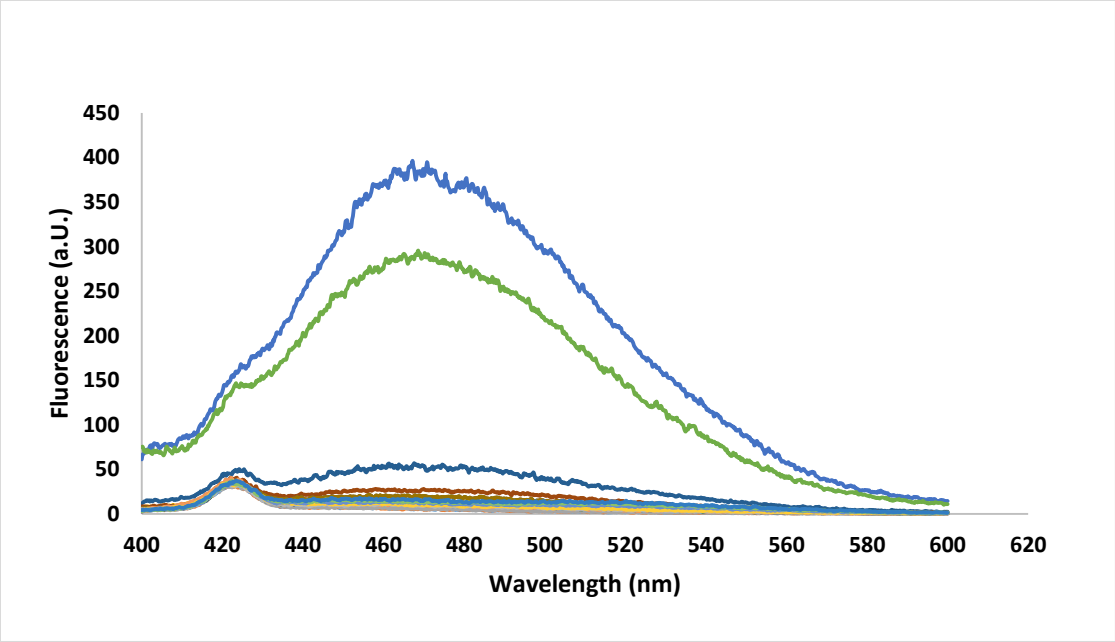

Figure 3.41. Sephadex G-75 chromatography of cell lysate treated with TCEP + TSQ. Reaction mixture of LLC-PK_1 cell lysate treated with TCEP then reacted with TSQ, was chromatographed through Sephadex G-75 gel filtration column, using degassed 20 mM Tris-Cl buffer pH 7.4. Fluorescence was recorded for each fraction.

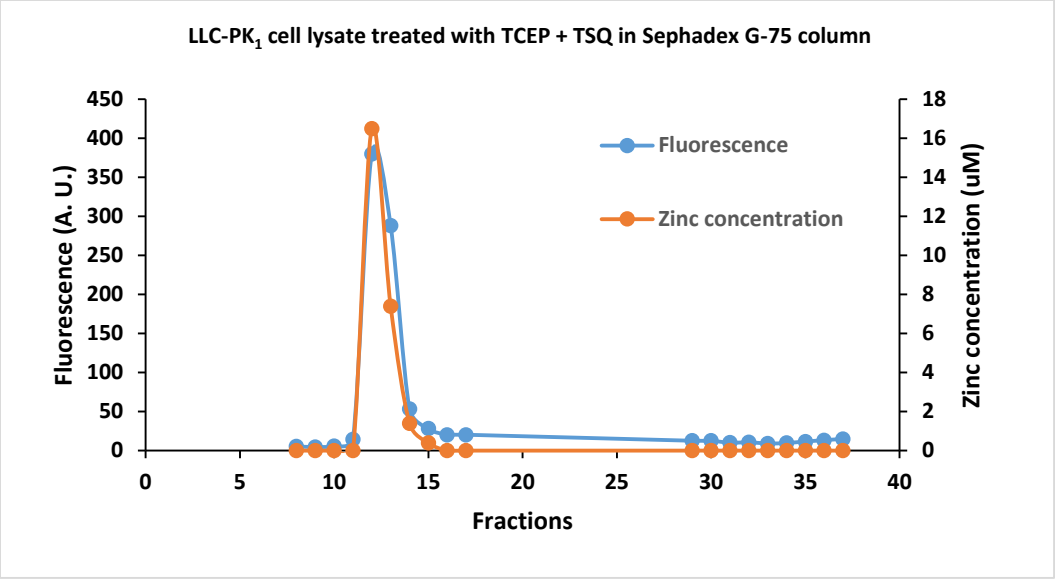

Figure 3.42. LLC-PK$_1$ cell lysate treated with TCEP + TSQ. The mixture was chromatographed using Sephadex G-75 gel filtration column, the fluorescence and Zn^{2+} concentration were recorded for the fractions eluted from the column.

Part-ii: *LLC-PK$_1$ cell lysate without TCEP*

The other one mL cell lysate mentioned above was directly titrated with TSQ with a total of 20 uM concentration in two separate additions to observe the maximum intensity of fluorescence emission. Again, the results demonstrated the ternary adduct formation with the emission maximum centered at 470 nm, Figure 3.43.

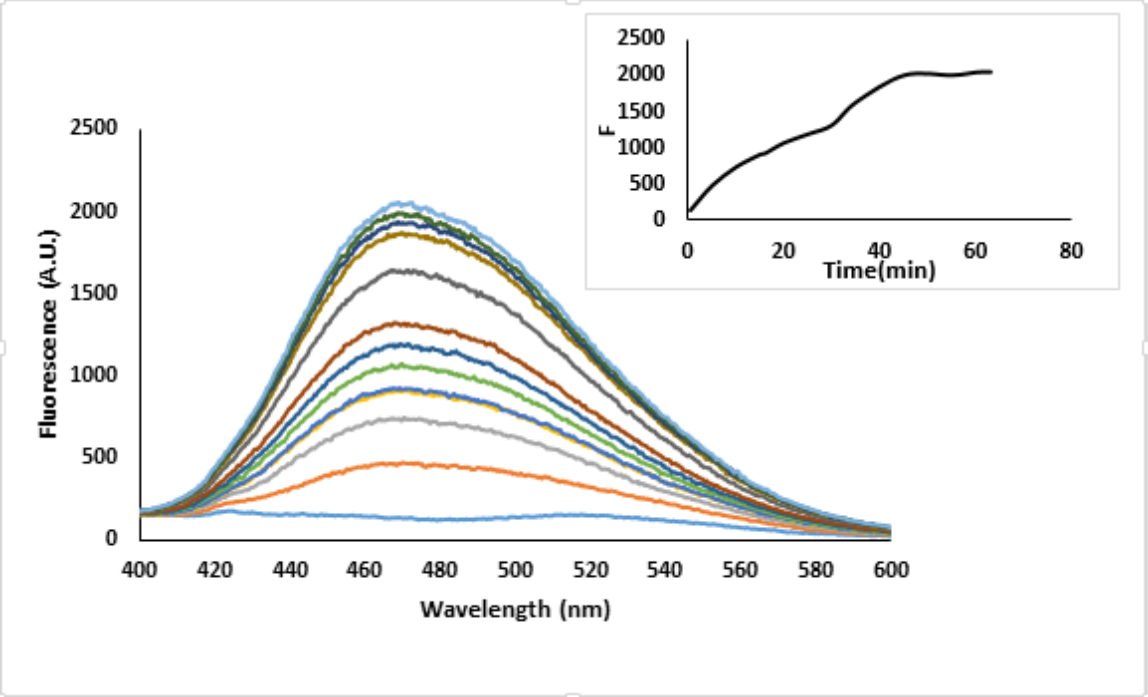

Figure 3.43. Fluorescence of LLC-PK$_1$ cell lysate + TSQ (without TCEP). One mL 10 uM of the LLC-PK$_1$ cell lysate was reacted with stepwise addition of total 20 uM TSQ and the fluorescence change was monitored over the time continued until 63 minutes.

Further the reaction mixture was eluted through Sephadex G-75 and 40 fractions each containing one mL were collected. The fluorescence data Figure 3.44 and the Zn^{2+} analysis Figure 3.45, both support that none has mobilized Zn^{2+} in LMW region, therefore Zn^{2+} is located at the HMW proteomic region.

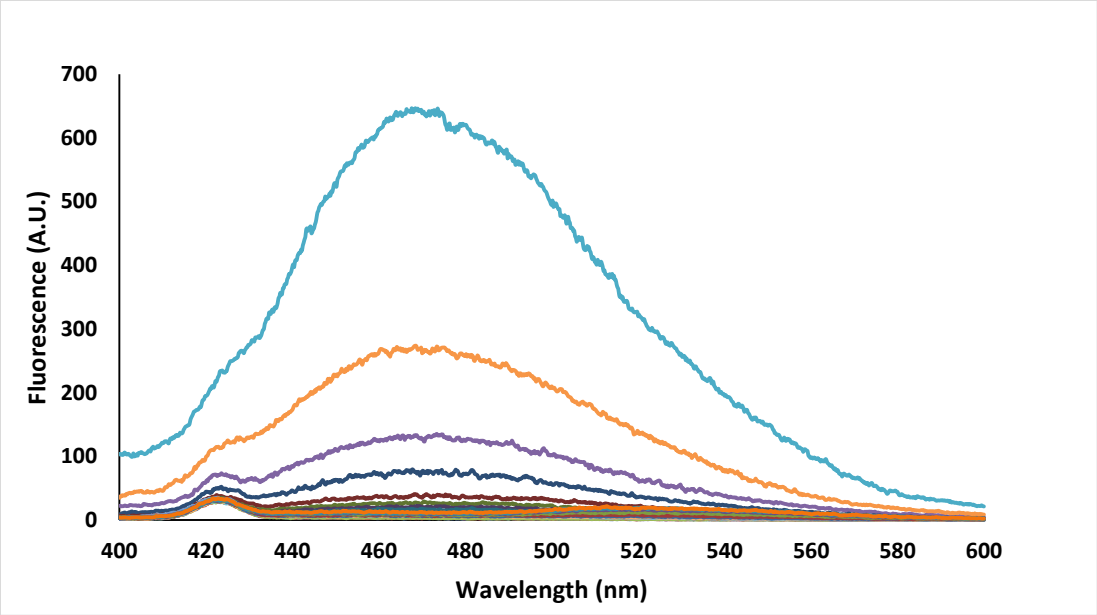

Figure 3.44. The LLC-PK1 cell lysate (without TCEP) + TSQ eluted in Sephadex G-75 gel filtration column. The reaction mixture was eluted in Sephadex G-75 column using degassed 20 mM Tris-Cl pH 7.4. The fractions were collected and the fluorescence was recorded for each fraction.

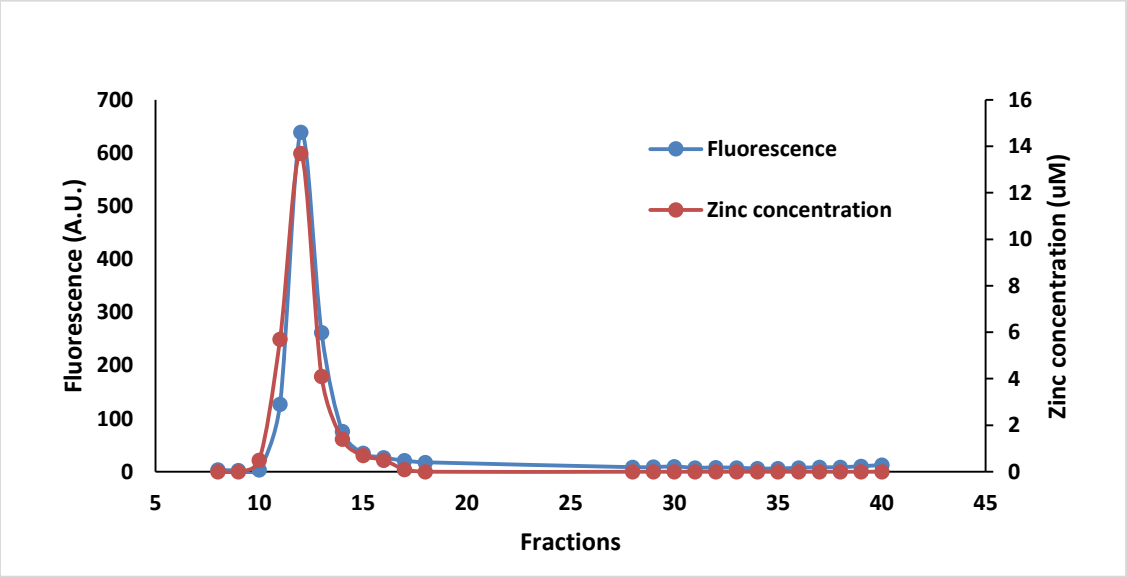

Figure 3.45. In Sephadex G-75 chromatography the reaction mixture of LLC-PK$_1$ cell lysate + TSQ was eluted. The fluorescence of the eluted fractions and the Zn^{2+} concentration were recorded.

Based on the data a comparison was made about the fluorescence intensity in Figure 3.40 and 3.43. Both the results of part-i and part-ii displayed above. A significant loss, about 40% of fluorescence intensity was observed and recorded for the cell lysate treated with TCEP. This result supports the hypothesis that TCEP protects glutathione against oxidation, limiting the availability of Zn-proteome to react with TSQ and resulting in lower fluorescence intensity.

To investigate this possibility again, experiments were repeated the model protein Alcohol Dehydrogenase (Section 3.8.2).

3.8.2. *Chemistry of TCEP with the model protein Alcohol Dehydrogenase*

A fresh solution of 17.5 uM Zn-ADH was prepared in 20 mM degassed Tris-Cl at pH 7.4. One mL of Zn-ADH was transferred in a cuvette and the fluorescence was recorded. Then the Zn-ADH solution was reacted with 35 uM of TSQ for 20 minutes, and the change in fluorescence intensity was monitored to determine when the maximum intensity was achieved. As expected ternary adduct formation at a blue shifted emission maxima centered at 470 nm was observed, (Figure 3.46). Subsequently, the mixture was titrated with increasing concentration of TCEP up to 1.18 mM of total concentration. The results displayed in Figure 3.47.

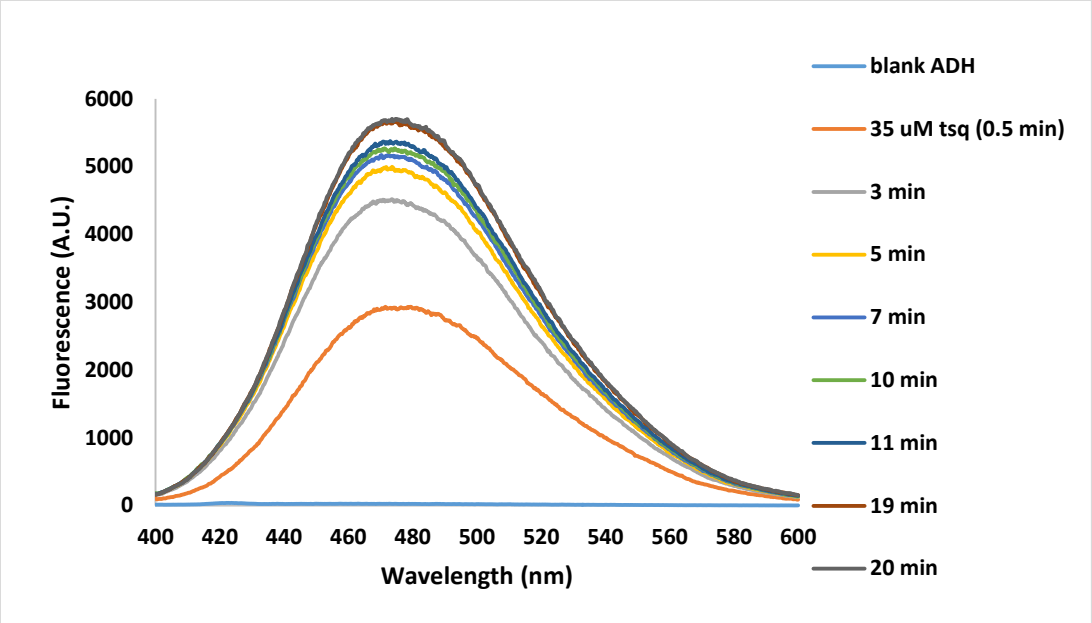

Figure 3.46. Titration of Zn-ADH with TSQ. 17.5 uM of Zn-ADH in 20 mM degassed Tris-Cl pH 7.4 was reacted with 35 uM TSQ over 20 minutes to obtain the maximum fluorescence spectrum.

The titration of Zn-ADH with TCEP did not show any significant fluorescence change. The titration was continued until 40 minutes. Thus, it was concluded that TCEP does not compete with TSQ for Zn bound to ADH.

Zn-ADH + TSQ ⇆ TSQ-Zn-ADH (3.25)

TSQ-Zn-ADH + TCEP ⇆ No reaction (3.26)

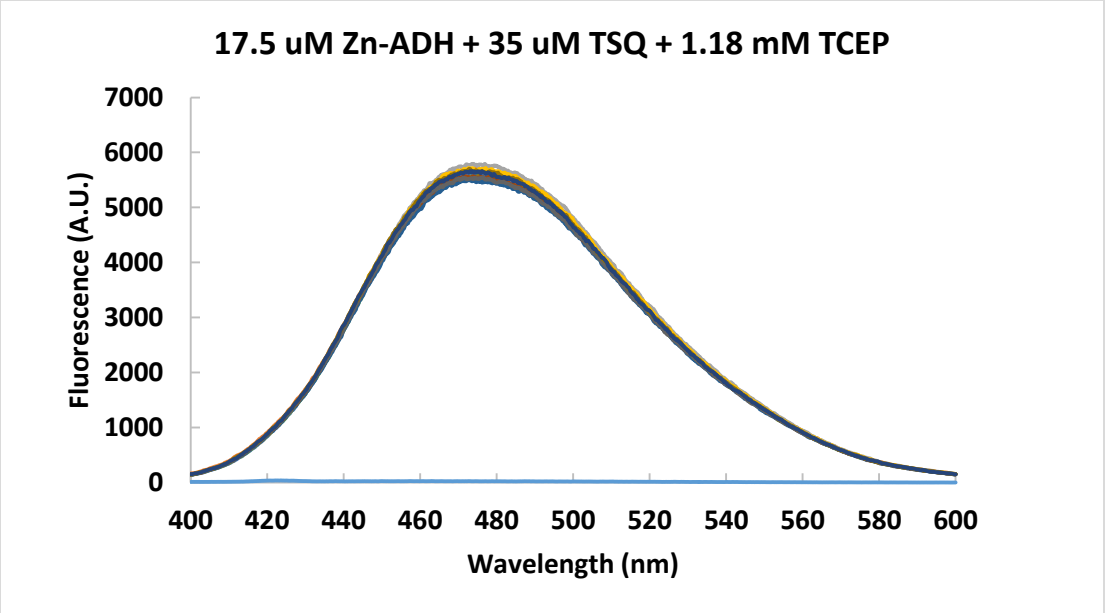

Figure 3.47. The adduct of TSQ-Zn-ADH titration with TCEP. 17.5 uM Zn-ADH was reacted with 35 uM TSQ then the adduct of TSQ-Zn-ADH was titrated with a total concentration up to 1.18 mM TCEP.

4. Discussion

The study of Zn-proteins and their function in human health and disease requires effective tools for zinc bioimaging. Such tools have recently focused on the use of fluorescent zinc sensors.[35,49,50,38] In spite of the rapid advances in zinc and all other metal ion sensing, however, the current available probes will need additional modifications and improvement to overcome several remaining challenges. Such remaining improvements include reagents with improved metal and oxidation-state specificity, brighter fluorescent turn-on responses, and targetability to specific subcellular locations. That would provide the ability to perform new types of molecular imaging experiments.[50] In addition to that, research using other biologically important small molecules may provide new insights into the functions of zinc proteins. The specific goal in this dissertation work was studying some small molecule ligands and their adduct formation with zinc proteins. The role of adduct formation between zinc proteins and biologically active small molecules may play a role in anti-tumor activity. Also the adduct formation with these non-fluorescent small molecules can lend new insight towards the study of zinc imaging.

1,10-phenanthroline and its copper complexes have been investigated for their roles in biological activities, such as anti-tumor, anti-*Candida*, anti-mycobacterial and anti-microbial effects. [51] A recent study undertaken by C. Deegan, provided the first thorough examination of the potential application of phenanthroline and its metal based complexes as novel therapeutic agents for the treatment of cancer.[52,40] Another group expanded this to include such aromatic N-containing ligands as pyridine and imidazole. 1,10-phenanthroline and its analogues have donor properties

that are somewhat similar to the purine and pyrimidine bases and are showing a promising role as antitumor agents.[51]

The work of this thesis is based on studies by the Petering group, which shows that the zinc fluorophore TSQ binds with the Zn-proteome, when it undergoes reaction both *in vitro* and *in vivo*.[1] Ternary adduct formation is indicated by increased fluorescent intensity and unique, altered wavelength maxima centered near 470 nm.[1] Similar results were observed when TSQ was incubated with the model protein Alcohol Dehydrogenase (ADH). The lack of a 490 nm peak emission wavelength ($Zn(TSQ)_2$) in the proteome system indicated that TSQ imaged the zinc proteome as a ternary adduct (TSQ-Zn-Proteome).[1,5] Therefore, the observed fluorescence (fluorescence microscopy or spectrofluorometry) of TSQ stained cells should be interpreted as the fluorescence of the TSQ-Zn-proteome, rather than assuming that there are pockets of free or labile zinc in the cells that react with TSQ to form $Zn(TSQ)_2$ as was hypothesized previously.[11,1] These pioneering results with TSQ were generalized by Dr. Andrew Nowakowski in 8 different cell lines. My research work replicated these results using the LLC-PK_1 cell line for the purpose of this thesis.

Experiments have been done to examine the hypothesis that biologically active metal binding ligands (L) such as 1,10-phenanthroline, the cellular tripeptide glutathione, some other multidentate ligands also bind as adducts to proteins in the zinc proteome. We used the following reactions to shed light on this topic and carry out the relevant experiments.

Zn-proteome + TSQ ⇆ TSQ-Zn-proteome (fluorescent) (4.1)

TSQ-Zn-proteome + L ⇆ L-Zn-Proteome + TSQ (non-fluorescent) (4.2)

In order to study the biologically active small molecules, TSQ-Zn-proteome was used as a reporter to evaluate whether competitive formation of non-fluorescent ternary adduct happens (see reaction 4.1 and 4.2).

The results show that 1,10-phenanthroline replaces most of the TSQ in a multiphasic manner. Figure 3.18 clearly shows that Phen did not mobilize (chelate) Zn^{2+} from the isolated Zn-proteome as the mechanism by which TSQ fluorescence is quenched. Thus the reaction results in the formation of Phen-Zn-proteome ternary adducts as Phen displaces TSQ from TSQ-Zn-proteome and quenches its fluorescence.

TSQ-Zn-proteome + 1,10-phenanthroline ⇆ Phen-Zn-proteome + TSQ (4.3)

Next, the capacity of the ligand 1,10-phenathroline to replace TSQ was tested *in vivo* using the pig kidney cell line LLC-PK_1 . It is evident from the results (Figure 3.10) that 1,10-phenanthroline is able to compete with TSQ in the intact cells as it does with the isolated Zn-proteome. Previous studies have suggested that Phen might sequester Zn from Zn-proteome or bind Fe or Cu in cells leading to redox reactions and the production of reactive oxygen species. [40] Any of these might be responsible for the observed cytotoxicity of Phen. The present study shows that reaction of Phen with the Zn-proteins can also occur forming a ternary adduct. Therefore, some of the biological effects of 1,10-phenathroline may be attributable to adduct formation with the Zn-proteins.

The Sephadex G-75 column separation chromatography of the reaction mixture, strongly support that Phen only competes to replace TSQ in the high molecular weight proteins. There was no fluorescence in the low molecular weight fractions. Moreover, no trace of Zn^{2+} was detected in the metal analysis experiment of those fractions (see Figure 3.17).

To support the validity of the results above, using the pig kidney cell line, LLC-PK_1 and its isolated Zn-proteome, the model protein alcohol dehydrogenase (ADH) was also used. Carrying out the same set of experiments with Zn-Alcohol Dehydrogenase, a well-defined Zn-protein, confirmed the idea that Phen makes ternary adduct formation replacing the zinc imaging fluorophore TSQ.

Zn-ADH + TSQ ⇄ TSQ-Zn-ADH (fluorescence at 470 nm) (4.4)

TSQ-Zn-ADH + 1,10- Phen ⇄ Phen-Zn-ADH + TSQ (reduced fluorescence) (4.5)

In light of the support for the hypothesis that the Zn-proteome can form adduct species with Phen, an additional experiment was carried out, involving enzyme activity assay. In the enzyme activity assay the conversion of NAD^+ to NADH was utilized to monitor the initial rate of catalysis. Upon additions of 50 uM and 80 uM 1,10-phenanthroline, the rate of the reaction was reduced 28% and 50%. The enzyme activity assay data brings forth the notion of the ability of 1,10-Phenanthroline to inhibit the enzyme Zn-Alcohol Dehydrogenase.

Finally, an experiment that supported Zn-proteome into individual proteins using NSDS-PAGE method. The proteome were then treated with TSQ and then with 1,10-phenanthroline, (Figure 3.33) to visualize adduct formation properties of 1,10-phenanthroline with distinct proteomic region. The TSQ treated Zn-proteome bands brightly fluoresce due to the formation of TSQ-Zn-

proteome (Figure 3.33A). After subsequent addition of 1,10-phenanthroline, the fluorescence decayed as Phen-Zn-proteome (Figure 3.33B), replaced TSQ-Zn-proteome.

Hence, the exposure of cells to Phen or other small molecule ligands to the whole proteome bear the potential to perturb the functions of proteins. This quenching mechanism indicates that the zinc sensor, TSQ, which partially saturates the Zn-proteome, may serve as a reporter for monitoring the capacity of small molecule metal-binding ligands to react with Zn-proteome and generate adduct species, L-Zn-proteome.

Another chapter of this thesis encompasses an important cellular ligand glutathione (GSH). Glutathione is a tripeptide, glu-cys-gly. It is typically present at high concentration level (1-10 mM) in cells and is thus both the most prevalent cellular thiol and the most abundant low molecular weight molecule.[46] In the cell, glutathione plays a crucial role as an antioxidant. It carries one sulfhydryl group in its structure (Figure 3.34). The sulfhydryl groups help to maintain the intracellular redox state and protect the cells against oxidative damage.[45] Our aim was to see if glutathione (GSH) being a small molecule and a tripeptide does have any properties of ternary adduct formation with the labile pool of zinc in the Zn-proteome.

We carried out experiments to image Zn-proteome with TSQ to form the adduct of TSQ-Zn-proteome (Figure 3.35) and titrated with GSH. The data of this experiment showed that GSH is able to form a ternary adduct of GS-Zn-proteome (Figure 3.36) with GSH replacing TSQ from the adduct of TSQ-Zn-proteome at a higher concentration (about 1.15 mM). This positive result led to experiments with LLC-PK_1 cell lysate.

The ligand tris(2-carboxyethyl)phosphine or TCEP is conventionally used in biochemical research studies for the protection of thiol (-SH) groups by preventing their oxidation. As such, it helps to maintain the structure and proper activity of many proteins.[48,53,54] Previous research studies with TCEP gives ample information that it maintains the thiol (-SH) rich proteins in their reduced state and it also helps in enhancing the rate of the reaction of cysteine-rich peptides.[55,56,57] We decided to study the effect of the addition of TCEP in the LLC-PK_1 cell lysate whether it helps to maintain GSH in its reduced state.

In order to understand the effect of TCEP in preserving thiols in the cell lysate in its native reduced state, a control experiment with Zn^{2+} solution was carried out. When 10 uM of Zn^{2+} was reacted with 10 uM TSQ it was observed that $Zn(TSQ)_2$ complex was formed and the emission wavelength being centered at 490 nm. When TCEP was reacted with the complex $Zn(TSQ)_2$ it was found that large concentration of TCEP can to a small extent replace TSQ from the $Zn(TSQ)_2$ complex forming a $Zn(TCEP)_2$ complex. This provided the initial evidence that TCEP is able to form the $Zn(TCEP)_2$ complex (see Figure 3.39).

Then the impetus was to investigate the effect of TCEP in the cell lysate. To understand that possibility we carried out experiments with LLC-PK_1 cell lysate. In the LLC-PK_1 cell lysate, not only are Zn-proteins available, but glutathione and other small molecular weight proteins are present. We followed up the idea of adduct formation of GSH with Zn-proteome (Figure 3.36). Because GSH is able to form ternary adduct with zinc in the Zn-proteome, it will be partially limiting the availability of Zn-proteome in the cell lysate to react with TSQ. Previous studies in our lab had shown that GSH undergoes oxidation once cells are lysed and the lysate is exposed to air. If TCEP protects the thiol (-SH) groups from being oxidized to GS-SG, then our expectation was to see lower fluorescence intensity when the LLC-PK_1 cell lysate was treated with TCEP. We found evidence to support this hypothesis from the data. The LLC-PK_1 cell lysate treated with TCEP was compared with data of LLC-PK_1 cell lysate not treated TCEP (Figure 3.40 and 3.43). The TCEP treated cell lysate revealed lower fluorescence intensity when incubated with TSQ compared to the non-treated cell lysate (Figure 3.40 and 3.43). Both sets of experiments were carried out at the same time keeping the same stoichiometry of the cellular environment, the reagents used, and the parameters in the fluorimeter (see chapter 2, part-i and part-ii).

In all of the experiments above, when the pool of the mixture containing adducts of GS-Zn-proteome and TSQ-Zn-proteome in the cell lysates were chromatographed over the Sephadex G-75 column, only the HMW proteome fractions displayed fluorescence and Zn^{2+} (Figure 3.42 and 3.45). There was neither fluorescence nor Zn^{2+} in the LMW fractions. These results lead to conclusion that GSH does make ternary adducts within the Zn-proteome in the cell lysate. However, we were not able to directly measure GSH concentration because TCEP interfered with the colorimetric reaction. Future experiments will need to determine GSH by another method.

Assuming our interpretation is correct, then GS-Zn-proteome complexes may exist in cells. Since many Zn^{2+} binding sites contain thiol ligands, directly bound GSH may be particularly effective protecting these sites from oxidation.

References:

1. Meeusen, J. W., Tomasiewicz, H., Nowakowski, A. & Petering, D. H. TSQ (6-methoxy-8-p-toluenesulfonamido-quinoline), a common fluorescent sensor for cellular zinc, images zinc proteins. *Inorg. Chem.* **50,** 7563–7573 (2011).

2. Andreini, C., Banci, L., Bertini, I. & Rosato, A. Counting the zinc-proteins encoded in the human genome. *J. Proteome Res.* **5,** 196–201 (2006).

3. Andreini, C., Banci, L., Bertini, I. & Rosato, A. Zinc through the three domains of life. *J. Proteome Res.* **5,** 3173–3178 (2006).

4. Haase, H. & Rink, L. Zinc signals and immune function. *BioFactors* **40,** 27–40 (2014).

5. Nowakowski, A. B. & Petering, D. H. Reactions of the fluorescent sensor, zinquin, with the zinc-proteome: Adduct formation and ligand substitution. *Inorg. Chem.* **50,** 10124–10133 (2011).

6. Tomat, E. & Lippard, S. J. Imaging mobile zinc in biology. *Curr. Opin. Chem. Biol.* **14,** 225–230 (2010).

7. Sensi, S. L., Paoletti, P., Bush, A. I. & Sekler, I. Zinc in the physiology and pathology of the CNS. *Nat. Rev. Neurosci.* **10,** 780–791 (2009).

8. Maret, W. Zinc biochemistry: from a single zinc enzyme to a key element of life. *Adv. Nutr.* **4,** 82–91 (2013).

9. Finney, L. a & O'Halloran, T. V. Transition metal speciation in the cell: insights from the chemistry of metal ion receptors. *Science* **300,** 931–936 (2003).

10. Flinn, J. M. *et al.* Enhanced zinc consumption causes memory deficits and increased brain levels of zinc. *Physiol. Behav.* **83,** 793–803 (2005).

11. Maret, W. & Li, Y. Coordination dynamics of zinc in proteins. *Chem. Rev.* **109,** 4682–4707

(2009).

12. Turner, a J. Exploring the structure and function of zinc metallopeptidases: old enzymes and new discoveries. *Biochem. Soc. Trans.* **31,** 723–727 (2003).

13. Maret, W. Metals on the move: Zinc ions in cellular regulation and in the coordination dynamics of zinc proteins. *BioMetals* **24,** 411–418 (2011).

14. Frederickson, C. J., Suh, S. W., Silva, D., Frederickson, C. J. & Thompson, R. B. Zinc and Health : Current Status and Future Directions Importance of Zinc in the Central Nervous System : The Zinc-Containing. *J. Nutr.* 1471–1483 (2000).

15. York, J. & Nunberg, J. H. A novel zinc-binding domain is essential for formation of the functional Junín virus envelope glycoprotein complex. *J. Virol.* **81,** 13385–13391 (2007).

16. Kelleher, S. L., McCormick, N. H., Velasquez, V. & Lopez, V. Zinc in Specialized Secretory Tissues: Roles in the Pancreas, Prostate, and Mammary Gland. *Adv. Nutr. An Int. Rev. J.* **2,** 101–111 (2011).

17. Loas, A., Radford, R. J. & Lippard, S. J. Addition of a second binding site increases the dynamic range but alters the cellular localization of a red fluorescent probe for mobile zinc. *Inorg. Chem.* **53,** 6491–6493 (2014).

18. Miao, X., Sun, W., Fu, Y., Miao, L. & Cai, L. Zinc homeostasis in the metabolic syndrome and diabetes. *Front. Med. China* **7,** 31–52 (2013).

19. Haase, H. & Rink, L. Multiple impacts of zinc on immune function. *Metallomics* **6,** 1175–80 (2014).

20. Ciavardelli, D. *et al.* Characterisation of element profile changes induced by long-term dietary supplementation of zinc in the brain and cerebellum of 3xTg-AD mice by alternated cool and normal plasma ICP-MS. *Metallomics* 1321–1332 (2012). doi:10.1039/c2mt20162c

21. Smith, M. a, Harris, P. L., Sayre, L. M. & Perry, G. Iron accumulation in Alzheimer disease is a source of redox-generated free radicals. *Proc. Natl. Acad. Sci. U. S. A.* **94,** 9866–9868 (1997).

22. Clements, A., Ailsop, D., Walsh, D. M. & Williams, C. H. Aggregation and Metal-Binding Properties of Mutant Forms of the Amyloid A ,@ Peptide of Alzheimer ' s Disease. 740–747 (1996).

23. Kepp, K. P. Bioinorganic chemistry of Alzheimer's disease. *Chem. Rev.* **112,** 5193–5239 (2012).

24. Andreini, C., Bertini, I. & Cavallaro, G. Minimal functional sites allow a classification of zinc sites in proteins. *PLoS One* **6,** (2011).

25. Manuscript, A. NIH Public Access. *Changes* **29,** 997–1003 (2012).

26. Ba, L. A., Doering, M., Burkholz, T. & Jacob, C. Metal trafficking: from maintaining the metal homeostasis to future drug design. *Metallomics* **1,** 292–311 (2009).

27. Truong-Tran, a Q., Carter, J., Ruffin, R. & Zalewski, P. D. New insights into the role of zinc in the respiratory epithelium. *Immunol. Cell Biol.* **79,** 170–177 (2001).

28. Raj, S. B., Ramaswamy, S. & Plapp, B. V. Yeast Alcohol Dehydrogenase Structure and Catalysis. *Biochemistry* (2014).

29. Vallee, B. L. & Auld, D. S. Cocatalytic zinc motifs in enzyme catalysis. *Proc. Natl. Acad. Sci. U. S. A.* **90,** 2715–2718 (1993).

30. Brandt, E. G., Hellgren, M., Brinck, T., Bergman, T. & Edholm, O. Molecular dynamics study of zinc binding to cysteines in a peptide mimic of the alcohol dehydrogenase structural zinc site. *Phys. Chem. Chem. Phys.* **11,** 975–983 (2009).

31. Dunn, F. & Mcfarlando, T. Dehydrogenase-Coenzyme Rates *. **252,** (1977).

32. Truong-Tran, a Q., Ruffin, R. E. & Zalewski, P. D. Visualization of labile zinc and its role in apoptosis of primary airway epithelial cells and cell lines. *Am. J. Physiol. Lung Cell. Mol. Physiol.* **279,** L1172–L1183 (2000).

33. Nolan, E. M. & Lippard, S. J. Small-molecule fluorescent sensors for investigating zinc

metalloneurochemistry. *Acc. Chem. Res.* **42,** 193–203 (2009).

34. Krebs, N. F. *et al.* Exchangeable zinc pool size in infants is related to key variables of zinc homeostasis. *J. Nutr.* **133,** 1498S–501S (2003).

35. Jiang, P. & Guo, Z. Fluorescent detection of zinc in biological systems: recent development on the design of chemosensors and biosensors. *Coord. Chem. Rev.* **248,** 205–229 (2004).

36. Frederickson, C. J., Kasarskis, E. J., Ringo, D. & Frederickson, R. E. A quinoline fluorescence method for visualizing and assaying the histochemically reactive zinc (bouton zinc) in the brain. *J. Neurosci. Methods* **20,** 91–103 (1987).

37. Varea, E., Ponsoda, X., Molowny, A., Danscher, G. & Lopez-Garcia, C. Imaging synaptic zinc release in living nervous tissue. *J. Neurosci. Methods* **110,** 57–63 (2001).

38. Nowakowski, A. & Petering, D. Sensor specific imaging of proteomic Zn2+ with zinquin and TSQ after cellular exposure to N-ethylmaleimide. *Metallomics* **4,** 448 (2012).

39. Nowakowski, A., Karim, M. & Petering, D. Zinc Proteomics. *Encycl. Inorg. Bioinorg. Chem.* 1–10 (2015). doi:10.1002/9781119951438.eibc2332

40. Kellett, A. *et al.* Radical-induced DNA damage by cytotoxic square-planar copper(II) complexes incorporating o-phthalate and 1,10-phenanthroline or 2,2'-dipyridyl. *Free Radic. Biol. Med.* **53,** 564–576 (2012).

41. Riss, T. L., Niles, A. L. & Minor, L. Cell Viability Assays Assay Guidance Manual. *Assay Guid. Man.* 1–23 (2004).

42. Sapan, C. V, Lundblad, R. L. & Price, N. C. Colorimetric protein assay techniques. *Biotechnol. Appl. Biochem.* **29 (Pt 2),** 99–108 (1999).

43. Nowakowski, A. B., Wobig, W. J. & Petering, D. H. Native SDS-PAGE: high resolution electrophoretic separation of proteins with retention of native properties including bound metal ions. *Metallomics* **6,** 1068–78 (2014).

44. Lee, J. Y., Kim, J. S., Byun, H. R., Palmiter, R. D. & Koh, J. Y. Dependence of the histofluorescently reactive zinc pool on zinc transporter-3 in the normal brain. *Brain Res.* **1418,** 12–22 (2011).

45. Wang, T., Lu, W., Lu, S. & Kong, J. Protective role of glutathione against oxidative stress in Streptococcus thermophilus. *Int. Dairy J.* **45,** 41–47 (2015).

46. Meister, a. Glutathione metabolism and its selective modification. *J. Biol. Chem.* **263,** 17205–17208 (1988).

47. Burns, J. a, Butler, J. C., Moran, J. & Whitesides, G. M. Selective reduction of disulfides by tris(2-carboxyethyl)phosphine. *J. Org. Chem.* **56,** 2648–2650 (1991).

48. Getz, E. B., Xiao, M., Chakrabarty, T., Cooke, R. & Selvin, P. R. A comparison between the sulfhydryl reductants tris(2-carboxyethyl)phosphine and dithiothreitol for use in protein biochemistry. *Anal. Biochem.* **273,** 73–80 (1999).

49. Thompson, R. B. Studying zinc biology with fluorescence: ain't we got fun? *Curr. Opin. Chem. Biol.* **9,** 526–32 (2005).

50. Domaille, D. W., Que, E. L. & Chang, C. J. Synthetic fluorescent sensors for studying the cell biology of metals. *Nat. Chem. Biol.* **4,** 168–175 (2008).

51. Deegan, C., McCann, M., Devereux, M., Coyle, B. & Egan, D. A. In vitro cancer chemotherapeutic activity of 1,10-phenanthroline (phen), [Ag2(phen)3(mal)]x2H2O, [Cu(phen)2(mal)]x2H2O and [Mn(phen)2(mal)]x2H2O (malH2=malonic acid) using human cancer cells. *Cancer Lett.* **247,** 224–33 (2007).

52. Schmitt, S. M. NIH Public Access. **17,** 1257–1267 (2013).

53. Krężel, A., Latajka, R., Bujacz, G. D. & Bal, W. Coordination properties of tris(2-carboxyethyl)phosphine, a newly introduced thiol reductant, and its oxide. *Inorg. Chem.* **42,** 1994–2003 (2003).

54. Conte, M. Lo & Carroll, K. S. the Chemistry of Thiol Oxidation and Detection. *Oxidative Stress Redox Regul.* 1–42 (2013). doi:10.1007/978-94-007-5787-5_1

55. Tsuda, S., Yoshiya, T., Mochizuki, M. & Nishiuchi, Y. Synthesis of Cysteine-Rich Peptides by Native Chemical Ligation without Use of Exogenous Thiols. *Org. Lett.* 150319094936004 (2015). doi:10.1021/acs.orglett.5b00624

56. Park, J. B. *et al.* Direct measurement of active thiol metabolite levels of clopidogrel in human plasma using tris(2-carboxyethyl)phosphine as a reducing agent by LC-MS/MS. *J. Sep. Sci.* **36,** 2306–2314 (2013).

57. Chen, S., Jiang, H., Wei, K. & Liu, Y. Tris-(2-carboxyethyl) phosphine significantly promotes the reaction of cisplatin with Sp1 zinc finger protein. *Chem. Commun.* **49,** 1226 (2013).